

COMPARATIVE TAPHONOMY OF DEEP-SEA AND SHALLOW-MARINE ECHINOIDS OF THE GENUS *ECHINOCYAMUS*

TOBIAS B. GRUN,^{1,2} MORANA MIHALJEVIĆ,^{3,4} AND GREGORY E. WEBB³

¹*Florida Museum of Natural History, University of Florida, Gainesville, Florida 32611 USA*

²*Department of Geosciences, University of Tübingen, 72074 Tübingen, Germany*

³*School of Earth and Environmental Sciences, The University of Queensland, St Lucia, QLD 4072, Australia*

⁴*Science Lab UZH, University of Zurich, 8057 Zürich, Switzerland*

email: tgrun@ufl.edu

ABSTRACT: The infaunal living clypeasteroid echinoid genus *Echinocyamus* is considered a model organism for various ecological and paleontological studies since its distribution ranges from the polar regions to the tropics, and from shallow-marine settings to the deep-sea. Deep-sea analyses of this genus are rare, but imperative for the understanding and function of these important ecosystems. During the 2012 Southern Surveyor expedition, 35 seamounts off the east coast of Australia were dredged in depths greater than 800 m. Of these, six dredges contained a total of 18 deep-sea *Echinocyamus* tests. The tests have been analyzed for taphonomic alterations including abrasion patterns, macro-borings, micro-borings, depressions on the test, test staining, test filling, encrustation, and fragmentation. Findings are interpreted in the context of the deep-sea setting and are compared to *Echinocyamus* samples from shallow-water environments. Results show that abrasion in deep-sea environments is generally high, especially in ambulacral and genital pores indicating that tests can persist for a long time on the seafloor. This contrasts with shallow-water *Echinocyamus* that show lower abrasion due to early test destruction. Macro-borings are present as single or paired holes with straight vertical profiles resembling *Lithophaga* borings. Micro-borings are abundant and most likely the result of sponge or fungal activity. Depressions on the tests, such as scars or pits, are likely the result of trauma or malformation during ontogeny. Test staining is common, but variable, and is associated with Fe/Mn oxidation and authigenic clays based on elemental analyses. Test filling occurs as loose or lithified sediment. Encrustation is present in the form of rudimentary crusts and biofilms. No macro-organisms were found on the tests. Biofilm composition differs from shallow-water environments in that organisms captured in the biofilm reflect aphotic conditions or sedimentation of particles from higher in the water column (e.g., coccoliths). Fragmentation is restricted to the apical system and pore regions. Results of this first comparative study on deep-sea *Echinocyamus* from Australian seamounts show that the minute tests can survive for a long time in these settings and undergo environmental specific taphonomic processes reflected in various taphonomic alterations.

INTRODUCTION

Taphonomic studies on echinoids have focused primarily on readily accessible shallow-water environments with depths less than 100 m (e.g., Kidwell and Baumiller 1990; Greenstein 1991, 1993; Nebelsick 1995; Dynowski 2012; Grun and Nebelsick 2016; Grun et al. 2017, 2018). Studies on echinoderms from the deep-sea are rare and mostly focus on crinoids and other echinoderms (e.g., Ausich 2001; Baumiller 2003; Gorzelak and Salamon 2013). Little work has been published on deep-sea echinoids (e.g. Deline and Parsons-Hubbard 2013).

Despite the lack of knowledge on deep-sea taphonomy in echinoids, taphonomic processes have been shown to be similar to those of the better-known shallow-marine environments (Walker and Voight 1994). Taphonomic processes in deep-sea environments, their effect on organism remains, timing and prevalence, however, differ as a result of various biological constraints and physical-chemical conditions. For example, the rate of sedimentation, which plays a very important and multi-faceted role in the taphonomic process (Sexton and Wilson 2009), is generally higher in shallow-marine environments than in the deep-sea. This can lead to delay in burial and prolonged exposure on the sea floor and potentially greater temporal mixing and time averaging of deep assemblages. Transport and

fragmentation of remains is decreased in deep-sea environments as a result of low water- and sediment agitation. Thus, taphonomic alteration in deep-sea environments may be higher compared to those of shallow marine settings.

The Shelf and Slope Experimental Taphonomy Initiative (SSETI) examined taphonomic rates for a variety of substrates, including carbonate skeletons, from 15 to 570 m depth (Parsons et al. 1997; Parsons-Hubbard et al. 2011). In comparing mollusk taphonomy over a 13-year interval during the SSETI, Brett et al. (2011) and Powell et al. (2012) noted significant differences in taphonomic rates between different habitats related to near surface pore water chemistry, especially carbonate mineral saturation levels and redox reactions, and sedimentation rates and highlighted the value of taphonomic information for environmental reconstruction. More recent work in the Azores reported analyses of calcareous epiliths from the intertidal zone to depths of 500 m (Wissak et al. 2015) and nautiloid taphonomy was documented to depths below 750 m (Tomašových et al. 2017).

Owing to the great value of deep-sea paleoclimate archives, intense work on deep-sea foraminifers has provided insights into taphonomic effects (Collen and Burgess 1979; Denne and Sen Gupta 1989; Freiwald 1995;

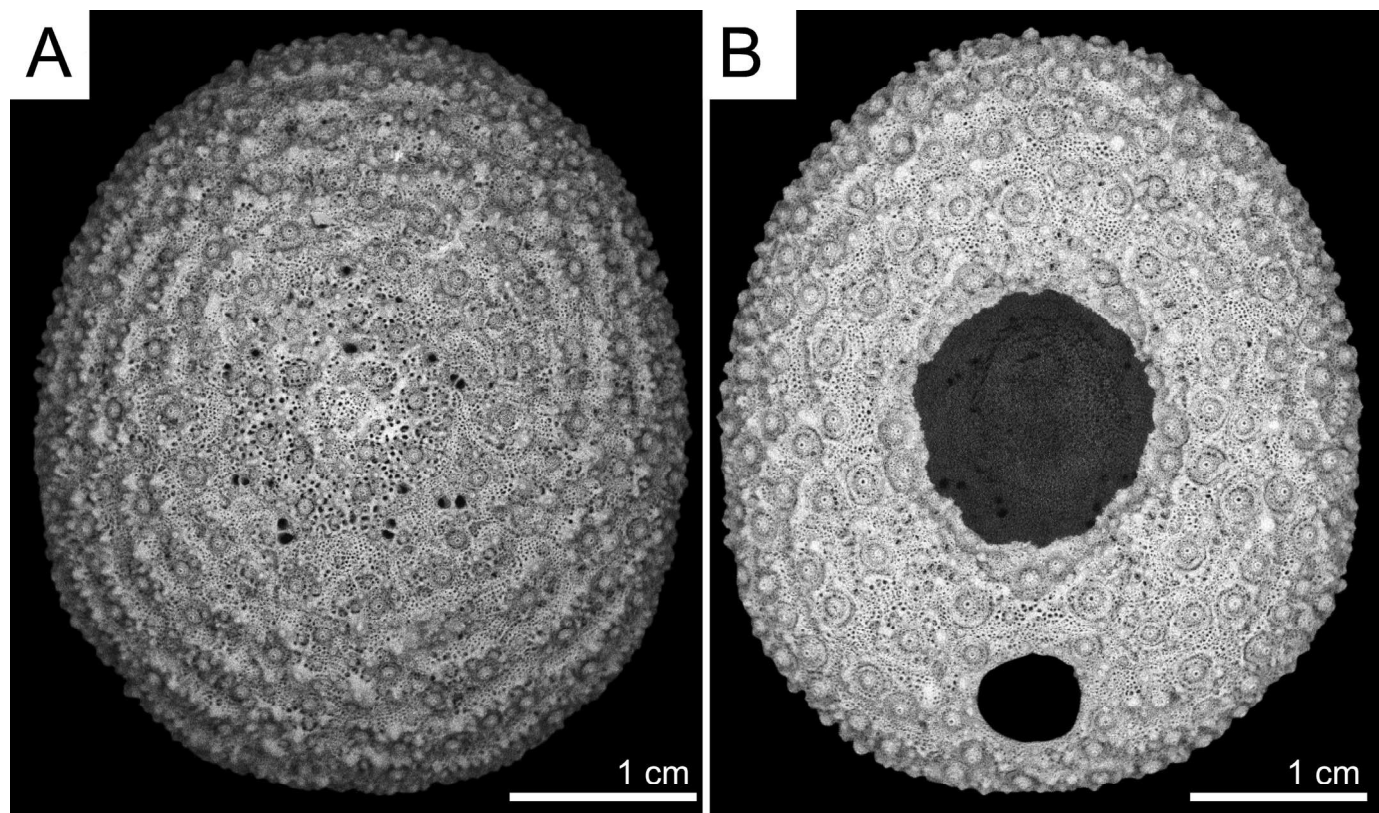


FIG. 1.—*Echinocyamus* specimen from deep-sea Tasmanid Seamount chain. A) Aboral view. B) Oral view.

Rathburn and Miao 1995; Brown and Elderfield 1996; Alve and Murray 1997; Murray and Alve 1999; Haley et al. 2005; Dawber and Tripati 2012; Tachikawa et al. 2013), significance as geochemical proxies (Cronblad and Malmgren 1981; Palmer and Elderfield 1986; Groeneveld et al. 2008; Sexton and Wilson 2009; Rongstad et al. 2017), and burial regimes of several hundred meters below the seafloor in some cases (e.g., Higgins and Shrag 2012; Bransen et al. 2015; Higgins et al. 2018). Deep-sea corals and coral mounds also have been increasingly studied for similar reasons (e.g., Freiwald and Wilson 1998; Beuck et al. 2007, 2010; Roberts et al. 2009; Van der Kooij et al. 2010; Stevenson and Rocha 2013). Micro-borings in carbonate skeletons have long been used as bathymetric indicators with particular differences between shallow phototrophic assemblages and deeper assemblages, which are dominated by light-independent taxa (Boekschoten 1966; Bathurst 1967; Swinnett 1969; Golubic et al. 1975, 1984; Vogel et al. 2000; Glaub et al. 2001; Wissak 2012). Relatively few studies have been done on deeper, aphotic boring assemblages (Golubic et al. 2019) and significant convergence between shallow and deep endolithic ichnotaxa provides complicates comparisons (Golubic et al. 2016). Even though echinoids are important ecosystem engineers in soft-bottom habitats (e.g., Nebelsick 2020), their taphonomic pathways are understudied, yet imperative for a detailed understanding of deep-sea ecology, marine processes, and the interpretation of the fossil record.

This study provides a first description of taphonomic patterns found in the deep-sea echinoid *Echinocyamus* (Fig. 1) from dredged sea mounts off the coast of Australia. To improve the knowledge about deep sea echinoid taphonomy, tests are described and analyzed for (1) abrasion, (2) macro-borings, (3) micro-borings, (4) depressions, (5) staining, (6) filling, (7) encrustation, and (8) fragmentation patterns. Results are compared to taphonomic patterns found in shallow-water *Echinocyamus* and interpreted in the context of differences and similarities of (1) test abrasion, (2) encrustation rates, (3) encrustation organisms, and (4) fragmentation rates.

METHODS

Studied Organism

The minute clypeasteroid genus *Echinocyamus* (Fig. 1) is generally smaller than 20 mm in length (Mortensen 1948), ovate in shape and dorsoventrally flattened with an infundibulated (funnel shaped) peristome. Tests possess 10 internal radial buttresses, an apical system with four gonopores, small basicoronal plates with interambulacral elements larger than ambulacral elements. The periproct is located on the posterior oral side (Mortensen 1948; Smith and Kroh 2011). This genus is first known from Eocene strata.

Studied Area and Sampling

During the 2012 Southern Surveyor expedition (Cohen et al. 2012), 35 dredges were obtained from nine Tasmanid Seamounts (Fig. 2) across 22.5°S to 29.8°S latitudinal range from depths greater than 800 m (Table 1). The Tasmanid Seamounts are a chain of ancient 35 to 10 My old (Quilty 1993; Crossingham et al. 2017) volcanoes, located 150 to 600 km off the east coast of Australia with a geographical range between 36°S to 22°S latitude. *Echinocyamus* bearing sediments were collected using a 20 cm diameter, closed-bottom tube for foraminiferal ooze and fine sediments, which collects surface sediments from the upper 30 cm generally when the dredging process starts. However, dredges potentially collected material over bathymetric ranges of 130 to 220 m. Denuded *Echinocyamus* tests were hand-picked from sediment samples.

Taphonomic Characteristics

To assess taphonomic alteration of *Echinocyamus* tests we analyzed patterns of (1) abrasion, (2) macro-borings, (3) micro-borings, (4)

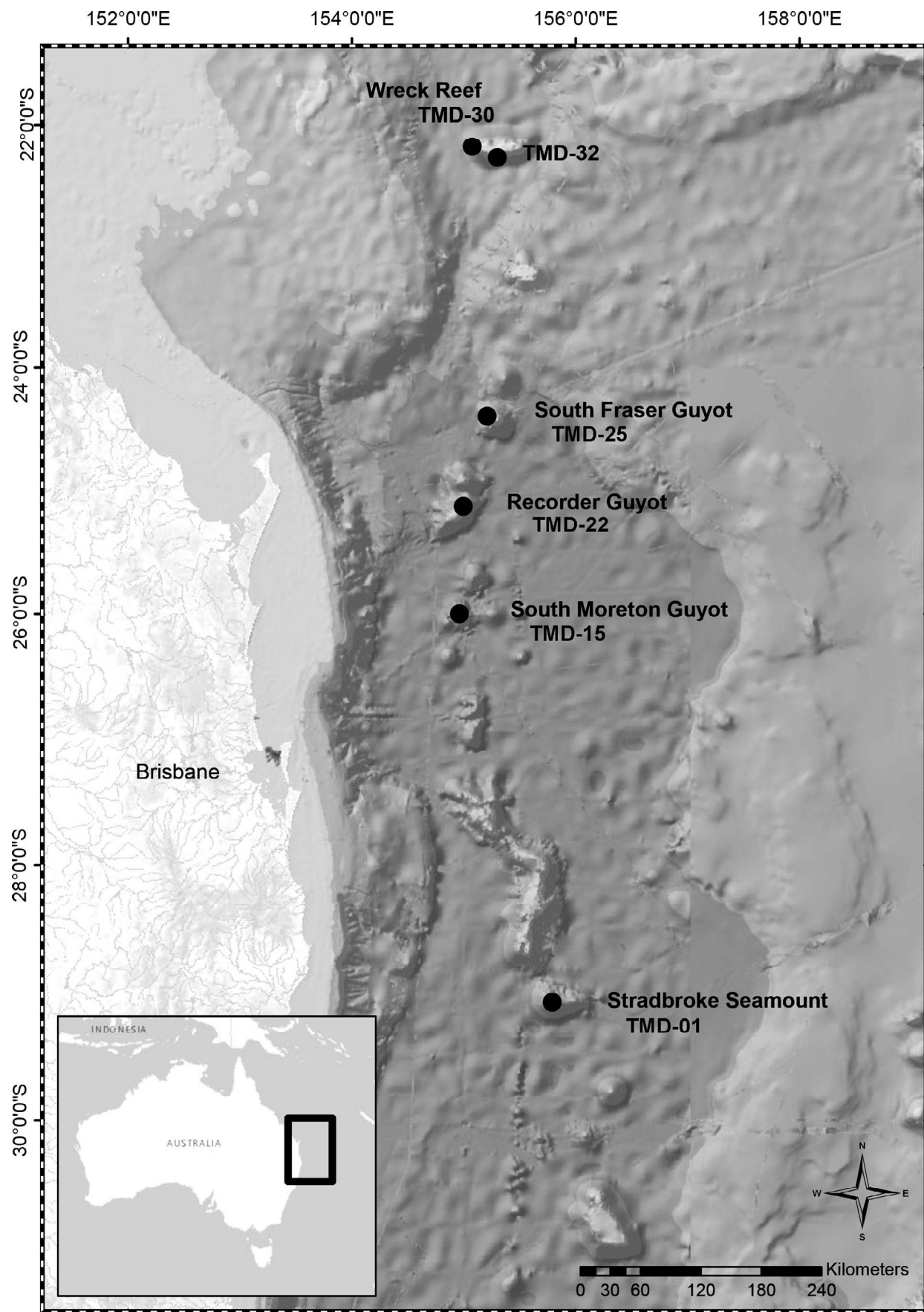


FIG. 2.—Map of Tasmanid Seamount dredging sites where *Echinocyamus* samples were collected. Inlay indicates the site relative to Australia (sourced from Google Earth 2017).

TABLE 1.—Dredge sites and details of *Echinocyamus* samples.

Dredge	Seamount	Coordinates	Depth (m)*	Total time in water	Total recovery	No. <i>Echinocyamus</i> individuals	Material recovered (Cohen et al. 2012)
TMD-01-SM294	Stradbroke Seamount	29°4.9' S 155°47.4' E	1460 [1250]	~ 2.5 h	300 kg	1	Volcanic rocks, limestone cobbles with fossil material, biota (deep-sea corals, sponges), foraminiferal ooze
TMD-15-SM241	South Moreton Guyot	26°0.5' S 154°57.8' E	1190 [970]	< 2 h	15 kg	1	Limestone cobbles, recrystallized coralliferous limestone, biota (deep-sea corals, gastropod), foraminiferal ooze
TMD-22-SM462	Recorder Guyot	25°7.8' S 154°59.9' E	1100 [880]	~ 2 h	70 kg	1	Limestone cobbles, recrystallized coralliferous, biota (deep-sea corals, mollusk, brachipods, crinoids), foraminiferal ooze
TMD-25-SM130	South Fraser Guyot	24°24.5' S 155°12.6' E	2330 [2130]	~ 2.5 h	40 kg	12	Limestone cobbles (rhodoliths within recrystallized bioclastic grainstone), a broken piece of volcanic rock, deep-sea sediments, and biota (deep-sea corals, barnacles, pteropods), foraminiferal ooze
TMD-30-SM463	Wreck Reef	22°11.2' S 155°4.5' E	1570 [1440]	~ 2 h	20 kg	1	Conglomerate with igneous cobbles, volcanoclastic sandstone, sandstone to conglomerate with carbonate matrix, biota (deep-sea corals, gastropods), foraminiferal ooze
TMD-32-SM388	Wreck Reef	22°16.3' S 155°18' E	2320 [2170]	~ 8 h	40 kg	2	Igneous rock types, both as rounded cobbles and as carbonate-cemented breccia, biota (mollusks and some shallow material including coral and <i>Halimeda</i> flakes apparently washed down from modern reef), foraminiferal ooze

* The foraminiferal ooze containing the described *Echinocyamus* was most likely collected in the deeper part of the range.

depressions, (5) staining, (6) filling, (7) encrustation, and (8) fragmentation. For comparability of abrasion grades, the protocol developed for shallow-water echinoids by Grun and Nebelsick (2016) was followed and extended (Table 2).

Abrasion.—Degrees of abrasion of the test surface, tubercles and pores were documented following the protocol developed by Grun and Nebelsick (2016) which is presented in detail in Table 2. Terminology follows Smith (1984).

Macro-Borings.—Macro-borings are defined as holes in the test that are clearly not the result of abiotic origin or fragmentation. These traces are characterized by sharp margins and are visible with the bare eye.

Micro-Borings.—Micro-borings are defined as open tubes that can be branched or unbranched, or small holes that are not visible with the bare eye.

Depressions.—Depressions are defined as deep, localized abrasions with sharp margins. These traces can be seen with the bare eye.

Staining.—Staining of the test can provide information on the local environmental chemistry and its exposure time under given conditions (Powell and Davies 1990; Best 2008). Three staining grades were defined including (1) light, (2) moderate, and (3) dark staining. To determine if test staining is based on an organic biofilm, two tests were bleached for 24 h in a solution of ~ 2.5% sodium hypochlorite. Stains also were investigated using an energy dispersive x-ray spectrometer (EDS) to determine elemental composition. In particular, a suite of eight samples showing increasing degrees of staining from a single dredge (TMD 25) were analyzed uncoated using a Hitachi TM3030plus scanning electron microscope (SEM) fitted with a Bruker EDS. An additional heavily stained (black) echinoid spine from the same dredge and a bleached test

fragment from a freshly dead shallow-water irregular echinoid were analyzed as staining endmembers on similar substrates. Analyses consisted of three circular 900 μm diameter spots per sample collected for 120 seconds at 15 kV on the aboral surface avoiding major pores, borings or other damage. Selected elements include C, O, Mg, Al, Si, Cl, Ca, Mn, and Fe. Although only pseudo-quantitative, normalization and quantification were carried out using integrated Quantax 70 software (Bruker). Post-analysis data manipulation was carried out using PAST software (version 3) (Hammer et al. 2001).

Filling.—Filling of the test can provide information on the burial conditions of the test. Three grades of filling have been defined: (1) not filled, (2) filled with unlithified sediment, and (3) filled with lithified sediment. ‘Lithified’ denotes that sediment cannot be loosened by shaking or tapping of the test.

Encrustation.—Encrustation is defined as biogenic material adhering to the test surface that generally leads to thickening of the test.

Quasimetric Method.—Following the protocol developed by Grun and Nebelsick (2016). Three alteration grades (grade 1, non-altered to slightly altered; grade 2, moderately altered; grade 3, highly altered) were defined for abrasion, fragmentation and encrustation (Table 2). A new character, glassy tubercles alteration, was added to the protocol (Table 2).

The proportion of each test surface affected by taphonomic alteration allowed assignment into five categories (category 1, taphonomic alteration not detectable; category 2, 0 to 25% of the area altered; category 3, 25 to 50% altered; category 4, 50 to 75% altered; and category 5, > 75% altered) (Grun and Nebelsick 2016). For category ‘test filling’ the proportions refer to proportion of the test filled with sediment. The only exception is the alteration category ‘staining’ where the test is visually assigned. For assessing total abrasion, fragmentation and filling, the quasimetric method of Grun and Nebelsick (2016) was followed (Table 3). Values for the five proportion

TABLE 2.—Test characters and their taphonomic alteration categories. Modified from Grun and Nebelsick (2016). Modifications are italicized. Asterisk indicates feature is comparable to “drillholes” in Grun and Nebelsick (2016).

Alteration	Character	Grade 1	Grade 2	Grade 3
Abrasion	tubercle	mamelon and boss present; mamelon can be partly abraded	boss present; mamelon entirely gone; boss can be partly abraded	stereom visible; mamelon and boss entirely gone; gap indicates former presence of tubercle
	surface and glassy tubercles	surface intact; no visible signs of abrasion; <i>glassy tubercles not abraded</i>	stereom can be slightly abraded; labyrinthic stereom not visible; <i>glassy tubercles partly abraded</i>	stereom abraded; labyrinthic stereom visible; <i>glassy tubercles gone</i>
	pores (oval also normal)	outline smooth; no visible signs of abrasion	outline irregular due to abrasion	outline ragged due to abrasion or fragmentation
Fragmentation	test	absent	cracks present	parts missing
Encrustation	test surface	absent	present	-
Macroborings*	borings outline (macroborings)	margins show no visible signs of abrasion	margins abraded	margins fragmented
	borings cross section (macroborings)	present	recognizable	not recognizable
Filling	<i>test cavity</i>	<i>absent</i>	<i>unlithified material</i>	<i>lithified material</i>
	<i>pores</i>	<i>absent</i>	<i>present</i>	-
Coloration	<i>test surface</i>	<i>none/white/light</i>	<i>medium</i>	<i>dark</i>

categories are: category 1, taphonomic alteration is virtually not detectable (value 0); category 2, up to 25% of the area or character is altered (value 1); category 3, 25 to 50% is altered (value 2); category 4, 50 to 75% is altered (value 3); and category 5, more than 75% of the area or character is altered (value 4). Abrasion values were calculated following the protocol developed by Grun and Nebelsick (2016) and are shown in Table 3.

Analyses.—The echinoids were analyzed using a reflecting stereo microscope (max. 10 \times magnification). Assigned scores were cross-checked by observing uncoated tests using a Hitachi TM3030 SEM in backscatter mode at low vacuum.

Taphonomic alteration of deep-sea samples was compared to shallow-water material analyzed by (Grun and Nebelsick 2016). These comparisons were not statistically evaluated because of the low number of deep-sea specimens (N = 18) and large difference in number of samples from the two environments (shallow-marine *Echinocyamus*, N = 1051). Although the deep-sea samples come from a relatively wide bathymetric range, and hence represent different local environments and sites, the aphotic deep ocean environment is less variable than shallower environments within the photic zone where light and energy gradients are much steeper and more variable both spatially and

temporally. Therefore, differences in our deep-sea sample sites might be less variable than differences shallow-water environments of a similar spatial distribution. Hence, our grouped data are considered to be indicative of the taphonomic differences between the broad environments.

RESULTS

A total of 18 *Echinocyamus* specimens were obtained from six dredges. These dredges started at water depths greater than 1000 m (Table 1). Four dredges contained a single, one dredge two tests, and another dredge 12 specimens. The other 29 dredges from depths greater than 800 m did not contain any *Echinocyamus* specimens or fragments. The degrees of taphonomic alteration ranged from almost pristine to highly altered tests (Table 4).

Abrasion

Total Abrasion.—Total abrasion values range from 1.1 to 2.6 (Table 4) with a mean of 1.45 ± 0.40 , N = 18. Total abrasion values are higher in deep-sea samples compared to shallow-water specimens (Fig. 3A).

TABLE 3.—Equations used for calculating total abrasion, fragmentation and infilling which followed the quasimetric approach described by Grun and Nebelsick (2016).

Total abrasion (V _A)	Total fragmentation (V _F)	Total filling (V _I)
$A_t = \frac{1P_{t1}+2P_{t2}+3P_{t3}}{P_{t1}+P_{t2}+P_{t3}}$	$V_F = \frac{1P_{F1}+2P_{F2}+3P_{F3}}{P_{F1}+P_{F2}+P_{F3}}$	$I_{ts} = \frac{P_{ts1}+2P_{ts2}+3P_{ts3}}{P_{ts1}+P_{ts2}+P_{ts3}}$
$A_s = \frac{1P_{s1}+2P_{s2}+3P_{s3}}{P_{s1}+P_{s2}+P_{s3}}$		$I_p = \frac{P_{p1}+2P_{p2}}{P_{p1}+P_{p2}}$
$A_p = \frac{1P_{p1}+2P_{p2}+3P_{p3}}{P_{p1}+P_{p2}+P_{p3}}$		$V_I = \frac{I_{ts}+I_p}{2}$
$V_A = \frac{A_t+A_s+A_p}{3}$		
A_t = tubercles	P_{F1} = proportion (categories 1 to 5) of non-altered tests surface	I_{ts} = infilling test
A_s = test surface	P_{F2} = proportion (categories 1 to 5) of fractures on the test surfaces	I_p = infilling pores
A_p = ambulacral and genital pores	P_{F3} = proportion (categories 1 to 5) of missing test parts	P_{ts} = proportion of test filled (categories 1 to 5) with different sediment types (grades 1 to 3)
P_t = proportion (categories 1 to 5) of altered tubercles (grades 1 to 3)		P_p = proportion (categories 1 to 5) of pores filled (grades 1 to 3)
P_s = proportion (categories 1 to 5) of altered test surfaces (grades 1 to 3)		
P_p = proportion (categories 1 to 5) of altered ambulacral and genital pores (grades 1 to 3)		

TABLE 4.—Overview of alterations in tests of deep-sea *Echinocyamus*. Abbreviations: A_t = tubercles; A_s = test surface; A_p = ambulacral and genital pores; V_A = total abrasion; V_F = total fragmentation; I_{ts} = filling test; I_p = filling pores; V_I = total filling; I_{type} = type of sediment filling the test.

Samples	A_t	A_s	A_p	V_A	Macroborning	Scars	V_f	Encrustation	I_{ts}	I_p	V_I	I_{type}	Coloration
TMD-1-SM294	1.2	1.2	1.83	1.41	absent	absent	1.4	absent	1	1.2	1.1	absent	moderate
TMD-15-SM241	2.6	2.8	2.33	2.58	absent	present	1.4	absent	1.8	1.8	1.8	lithified	dark
TMD-22-SM462	1.6	1.4	1.4	1.47	absent	absent	1	absent	2.6	1.4	2	lithified	dark
TMD-25-SM130-1	1	1.4	1.2	1.2	absent	present	1	absent	1	1.8	1.4	absent	light
TMD-25-SM130-2	1.2	1.2	1.2	1.2	present	absent	1	absent	1	1.2	1.1	absent	light
TMD-25-SM130-3	1.2	1.2	1.4	1.27	absent	absent	1	absent	1	1.4	1.2	absent	moderate
TMD-25-SM130-4	1.2	1.2	1.4	1.27	absent	absent	1	absent	1	1.2	1.1	absent	light
TMD-25-SM130-5	2.57	2.2	1.67	2.15	absent	absent	1.4	absent	1	1.4	1.2	absent	dark
TMD-25-SM130-6	1.2	1.2	1.2	1.2	absent	absent	1.4	absent	1	1.2	1.1	absent	light
TMD-25-SM130-7	2	2.6	1.2	1.93	absent	absent	1	absent	1	1.2	1.1	absent	dark
TMD-25-SM130-8	1.2	1.2	1	1.13	absent	absent	1	absent	1.4	1.33	1.37	lithified	light
TMD-25-SM130-9	1.5	1.2	1.4	1.37	absent	absent	1	absent	1.4	1.2	1.3	lithified	moderate
TMD-25-SM130-10	1.2	1.2	1.2	1.2	absent	absent	1	absent	1	1.4	1.2	absent	moderate
TMD-25-SM130-11	1.5	1.2	1.6	1.43	present	absent	1	absent	1.6	1.6	1.6	unlithified	light
TMD-25-SM130-12	1	1	1.2	1.07	absent	absent	1	absent	1.4	1	1.2	lithified	light
TMD-30-SM463	1.6	1.8	1.6	1.67	absent	absent	1	absent	1	1.2	1.1	absent	moderate
TMD-32-SM388-1	1.2	1.2	1.4	1.27	absent	present	1.4	absent	1.4	1.6	1.5	lithified	light
TMD-32-SM388-2	1.4	1.2	1.4	1.33	absent	absent	1	absent	1	1.2	1.1	absent	light

Surface Abrasion.—Test surface abrasion values range from 1.2 to 2.8 with a mean of 1.47 ± 0.53 , $N = 18$. The test surfaces range in preservation from completely intact to specimens where the outer stereom layers are abraded and the core-stereom exposed (Fig. 4).

Tubercle Abrasion.—Tubercle abrasion values range from 1.2 to 2.6 with a mean of 1.47 ± 0.47 , $N = 18$. Tubercles show various grades of abrasion with the mamelons and bosses being well-preserved to completely abraded (Fig. 4) compared to nearly unaltered tubercles (Fig. 5). Glassy tubercles show similar abrasion patterns as the spine-bearing tubercles.

Pore Abrasion.—Abrasion values of ambulacral pores and genital pores range from 1.2 to 2.3 with a mean of 1.42 ± 0.31 , $N = 18$. The pore edges can be sharply defined, slightly ragged or broken (Fig. 6).

Macro-Borings

Macro-borings were observed in two specimens belonging to the sample with 12 specimens (Figs. 7, 8A). The borings are subcircular to elongated holes, in some cases where close together, merging and resulting in a

figure-eight shape (Gibson and Watson 1989). Specimen TMD-25-130-2 contains two penetrating borings that are restricted to the oral side and range between 1.18 and 0.86 mm in length and are 0.29 mm in width on the narrowest part (Fig. 7A). The two borings are connected on their proximal ends and reach into the peristome. The boring profile is cylindrical in section with clearly defined margins that are not interrupted by surface structures, such as tubercles, glassy tubercles, or pores.

Micro-Borings

Micro-borings are common in the analyzed deep-sea specimens and may occur as filamentous, scalloped galleries (Fig. 9). These traces can be short, less than 10 μm in length, or span several hundred microns. Micro-borings generally occur in large quantities and proceed in a curved path. In some cases, the borings erode a large volume of the echinoid's stereom (Fig. 9D).

Depressions

Depressions occur exclusively on the test's surface of three specimens (Fig. 7B, 7C). They are restricted to the apical system (specimen TMD-25-

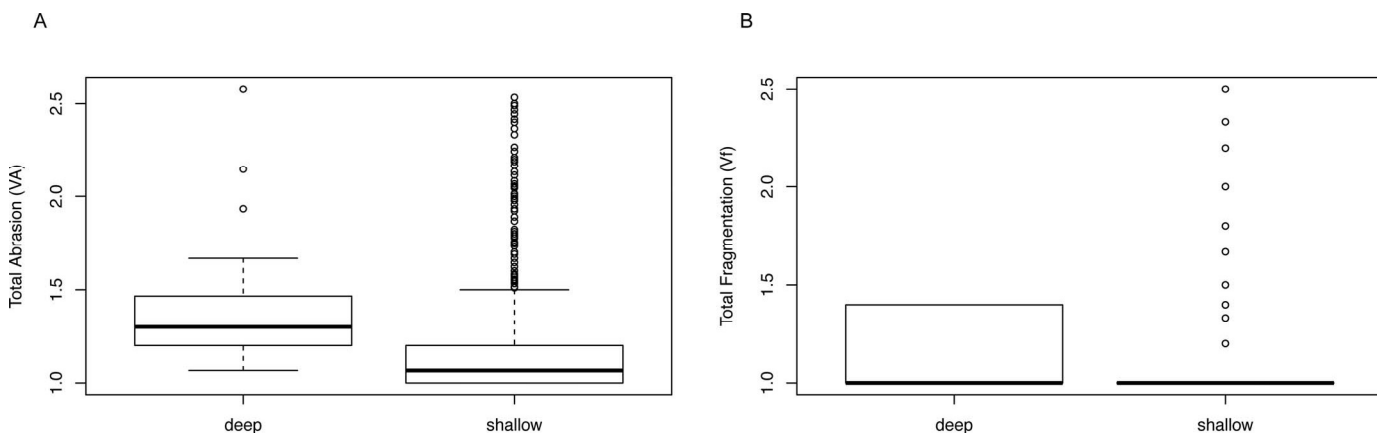


FIG. 3.—Box-plot comparison of deep-sea and shallow-water specimens of *Echinocyamus*. A) Total abrasion values are higher in deep-sea settings than in shallow-water environments. B) Range of fragmentation is narrower in deep-sea settings than in shallow-water environments.

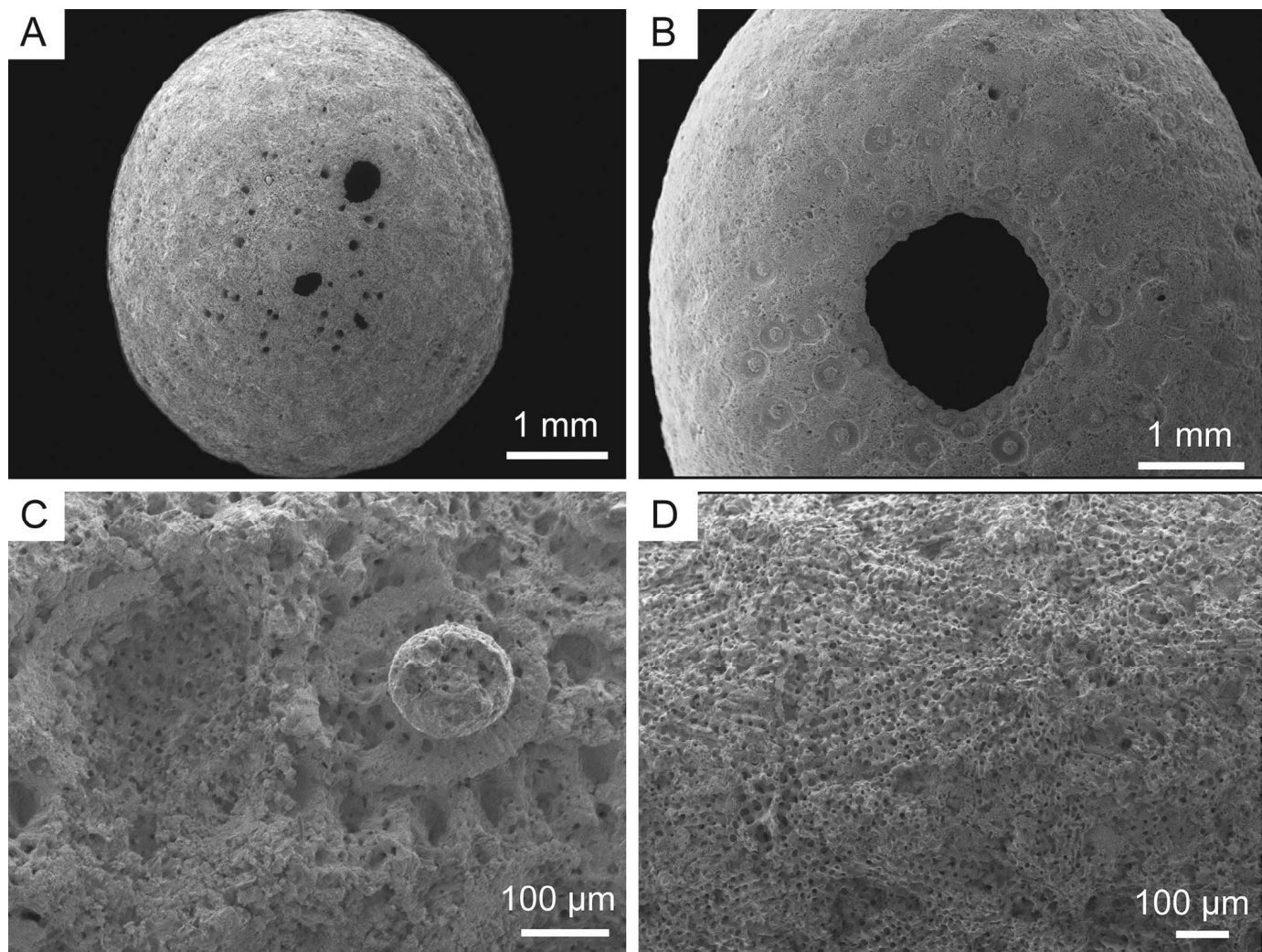


FIG. 4.—SEM images of taphonomically altered surface characters of *Echinocymus* specimens from the Tasmanid Seamounts. **A**) Overview of a highly abraded specimen (TMD-25-SM130-5) in aboral view. **B**) Detail view on the oral side of a test (TMD-15-SM241) where most of the surface characters are already gone. **C**) Two sunken tubercles in detail view. The left tubercle is gone leaving a pit behind, the right tubercle shows signs of abrasion in the mamelon, platform, boss, and areole (specimen TMD-22-SM462). **D**) Test surface is abraded exposing the underlying stereom (specimen TMD-25-SM130-5).

SM130-1) and the ambitus (specimens TMD-15-SM130-1 and TMD-32-SM388-1). The depressions vary in length but never penetrate the test. A scar located at the ambitus (Fig. 7C) in specimen TMD-25-SM130-11 appears to follow the figure-eight shape (Gibson and Watson 1989), but is not penetrating. The length of this trace is 0.41 mm in length and 0.03 mm at its narrowest part.

Staining

Nine of the 18 collected tests did not show significant staining. Moderate yellowish to brown staining (Fig. 10) was observed in five specimens. Four specimens showed darker brown test staining. Tests with darker staining were in some cases covered by a very thin (< 10 μ m thick) biofilm. Bleaching of biofilm covered tests did not remove the stain. Surface elemental analysis showed that the tests are dominantly composed of O, Ca, C, and Mg, consistent with high-Mg calcite, as expected, but staining is associated consistently with increased Mn, Fe, Si and Al (Fig. 11) (see Online Supplemental File for data and correlations). Including standard end-members, Mn and Fe are significantly correlated (Pearson's $r = 0.98$, $N = 30$, $p < 0.001$) with mean Mn reaching ~ 0.5 % (atomic) in

the most stained *Echinocymus* sample, but are less so among the eight test samples (Pearson's $r = 0.72$, $N = 24$, $p < 0.001$). Mean Si concentration reaches > 1.5 % (atomic) in the most stained *Echinocymus* sample and Si and Al are significantly correlated with and without standard end-members (Pearson's $r = 0.98$, $N = 30$, $p < 0.001$ and $r = 0.96$, $N = 23$, $p > 0.001$, respectively) whereas Fe and Si are less well correlated (Pearson's $r = 0.66$, $N = 24$, $p < 0.001$ without endmembers). Specimens with dark staining have the highest degree of total abrasion and fragmentation (Fig. 12A, 12B) but staining grade is not related to the frequency of macroboring, depressions or encrustation (Fig. 13).

Filling

Seven *Echinocymus* tests were filled to some degree by sediment. In six specimens, the sediment was lithified, one specimen was filled with unlithified sediment, and eleven specimens had no filling at all (Fig. 8). Lithification was variable, mostly being poorly lithified, but filling from sample TMD-25-SM130-8 is lithified in part by rhombic calcite cement (Fig. 8C). The filling sediment consists of foraminiferal ooze. There is no relationship between the staining and filling of the test and lithification

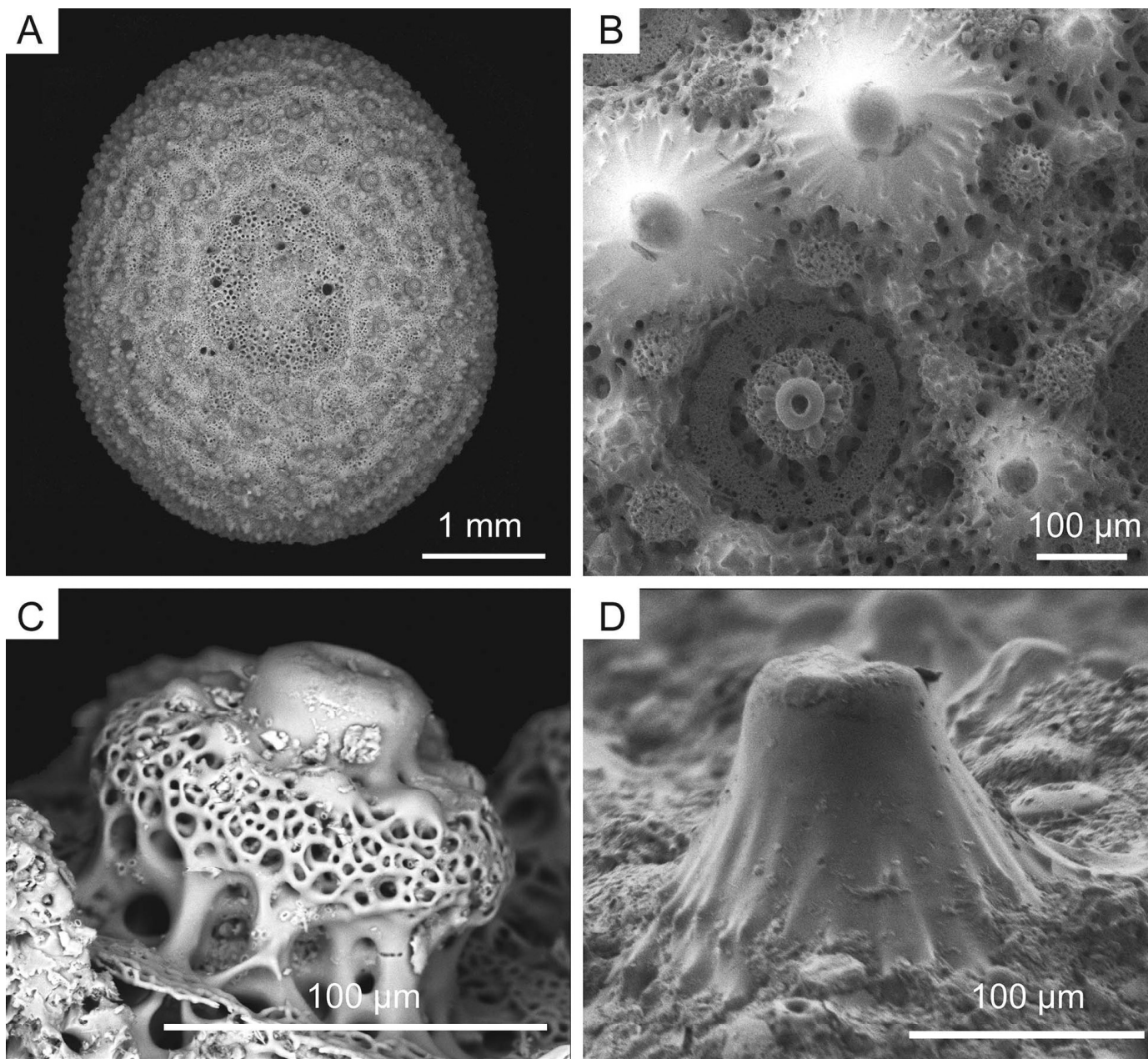


FIG. 5.—SEM images of well-preserved *Echinocyamus* from the Tasmanid Seamounts. **A**) Test in aboral view (specimen TMD-25-SM130-12). Tubercles and gonopores are well-visible. **B**) Sunken tubercle and protruding glassy tubercle in overview (specimen TMD-25-SM130-4). **C**) Sunken tubercle in detail view, all tubercle characteristics are well-preserved (specimen TMD-25-SM130-6). **D**) Well-preserved glassy tubercle in detail view (specimen TMD-32-SM388).

grade between the individuals (Fig. 14). Filling grade does not have an impact on the total abrasion or fragmentation (Fig. 13C, 13D). Sediment filling level is not related to the frequency of macroboring, depressions or encrustation.

Encrustation

Encrusting macro-organisms were not observed on any of the 18 specimens. However, two tests contained traces of encrustation (Fig. 15). An aggregation of elongate crystals that morphologically resemble aragonite on specimen TMD-25-SM130-6 is interpreted as remains of a holdfast of an encrusting organism (Fig. 15A). On the aboral surface of specimen TMD-25-SM130-3, a tube that penetrates the test is visible (Fig.

15B). Some of the tests are coated in a thin biofilm that trapped fine sediment, especially coccoliths, which are well preserved on the test's surface (Fig. 15C, 15D).

Fragmentation

Fragmentation occurred in three specimens and is restricted to plate loss of the apical system. Fragmentation where larger parts of the test are missing, was not observed. Furthermore, no evidence of plate or sutural fractures were noticed in the *Echinocyamus* tests. The total fragmentation value ranges from 1.0 to 1.4 with a mean of 1.11 ± 0.18 , $N = 18$. Abrasion is higher in individuals that experienced fragmentation (Fig. 16).

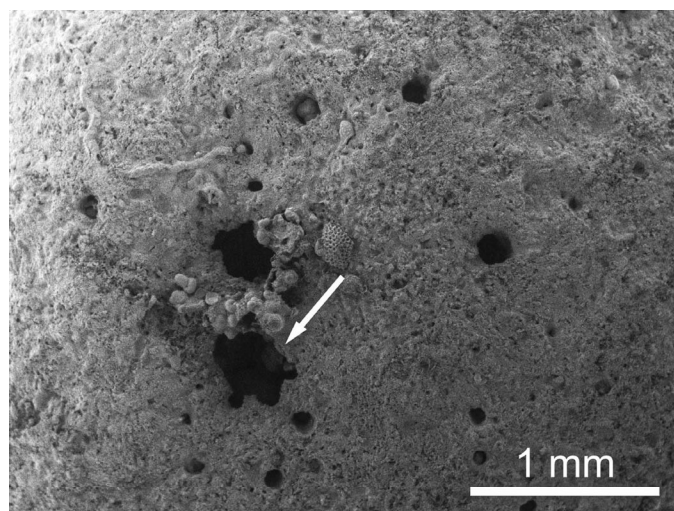


FIG. 6.—SEM image of *Echinocyamus* in aboral view. Arrow points to high abrasion around accessory pores (specimen TMD-15-SM241).

Fragmentation in deep-sea settings is lower compared to shallow-water samples (Fig. 3B).

DISCUSSION

Recent dredge samples from the Tasmanid Seamount chain in the Coral Sea off eastern Australia revealed previously undescribed deep-sea (900 to 2200 m) irregular echinoid specimens of the genus *Echinocyamus*. The 18 deep-sea specimens provide a first insight into taphonomic alteration in the minute echinoid genus *Echinocyamus* from deep-sea environments. Comparison of the deep-sea data to taphonomic analyses from shallow-water environments allows evaluation of differences and similarities in these two broadly defined environments.

Abrasion

Abrasion values among the deep-water samples are similar across the analyzed test features, including the test surface, tubercles and pores with abrasion values ranging from 1.4 to 1.5 with a total abrasion value of 1.45. These abrasion values indicate that abrasion acts at similar rates over the echinoid's test. Grun and Nebelsick (2016) reported total abrasion values for *Echinocyamus* tests from shallow-marine environments to be much smaller than those found in our deep-sea material (Fig. 3A) with total

abrasion values along sample sites ranging between 1.05 and 1.28. The authors concluded that highly abraded tests are likely to disintegrate in the high-energy settings leading to a bias that favors preservation of unabraded tests.

Abrasion of the test surface and tubercles are similar between deep-sea samples and the shallow-water environments. Deep sea samples, however, show higher pore abrasion than in the shallow-water samples reported by Grun and Nebelsick (2016). Pore margins can be abraded through the increased water flow and transport of fine deep-sea sediments through the pore opening. The higher pore abrasion in deep-sea samples indicates that these tests were exposed longer to the environment without being destroyed by currents or water agitation.

Macro-Borings

Macro-borings found in the deep-sea material (Figs. 7, 8) are distinct from previously reported predatory or parasitic borings for *Echinocyamus*, such as those of predatory cassid or parasitic eulimid gastropods (e.g., Nebelsick and Kowalewski 1999; Złotnik and Ceranka 2003; Grun et al. 2014, 2017). Boreholes in *Echinocyamus* previously were described as circular to subcircular featuring a cylindrical (Nebelsick and Kowalewski 1999) or concave (Grun et al. 2014) vertical profile. These reported borehole morphologies are strongly affected by the microstructure of the skeleton, such as tubercles and pores (Grun et al. 2014). Macro-borings in the deep-sea specimens (Figs. 7A, 8A) are subcircular with a cylindrical profile, but commonly occur in pairs, which can result in figure-eight shaped traces (Gibson and Watson 1989). Macro-borings are not affected by the skeletal microstructures of *Echinocyamus*, which contrasts with predatory gastropod borings. The figure-eight shaped traces found in the deep-sea *Echinocyamus* samples resembles boreholes produced by the boring bivalve *Lithophaga* (e.g., Jones and Pemberton 1988, Belaústequi et al. 2012) or predatory nematodes (e.g., Lipps 1983). The latter, however, is on a much smaller scale and can thus be excluded.

Micro-Borings

Micro-borings (Fig. 9) were recorded only from the test surface and within the stereom of the deep-sea *Echinocyamus* tests. These borings are probably caused by sponges, fungi or other lithophagous micro-organisms (e.g., Beuck et al. 2010; Golubic et al. 2019). Although not mentioned by Grun and Nebelsick (2016), micro-borings also were present in *Echinocyamus* from the shallow-water environments (Grun and Nebelsick 2016, fig. 3). In shallow-water settings, such micro-borings commonly are produced by cyanobacteria and boring algae and can be very abundant (e.g., Chazottes et al. 2009). Bioerosion on *Echinocyamus* tests from deep-

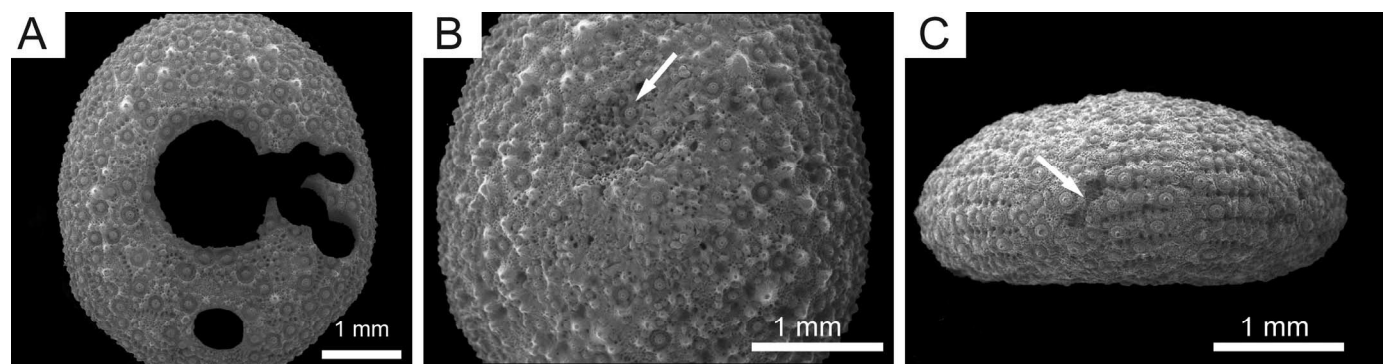


FIG. 7.—SEM images of macro-borings and depressions in *Echinocyamus* tests from the Tasmanid Seamounts. A) Figure-eight macro-boring on the oral surface (specimen TMD-25-SM130-2). B) Arrow points to depression (pit) on the aboral side of the test (specimen TMD-25-SM130-1). C) Arrow points to scar on the ambitus (specimen TMD-25-SM130-11).

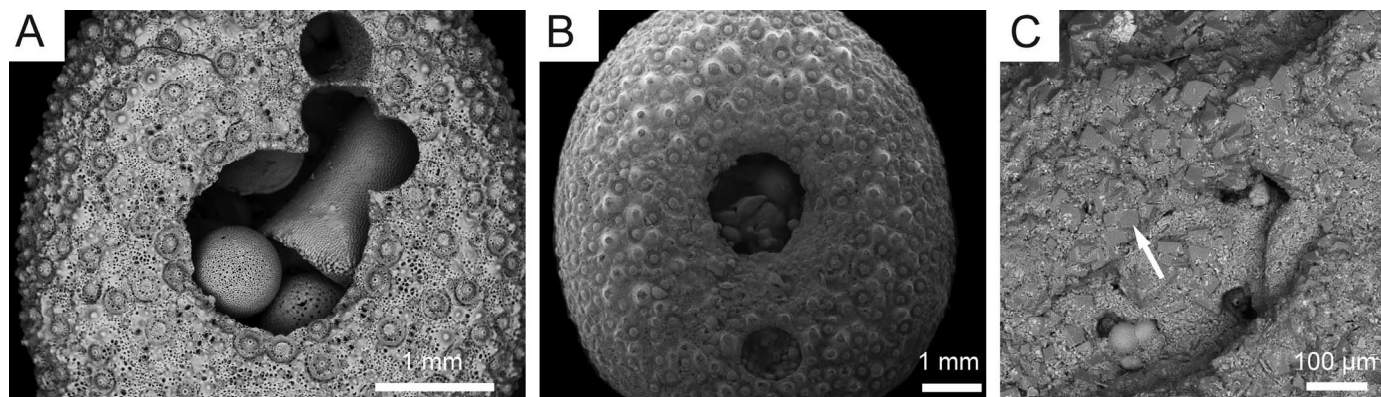


FIG. 8.—SEM images of macro-borings and sediment fillings of *Echinocyamus* tests from the Tasmanid Seamounts. **A**) Oral view with single macroboring and a paired figure-eight boring. Test (TMD-25-SM130-11) is filled with unlithified sediment. **B**) Oral view of a test (TMD-22-SM462) with lithified filling. **C**) Oral view of a test (TMD-25-SM130-8). Arrow points to rhombic calcite crystals cementing the filling.

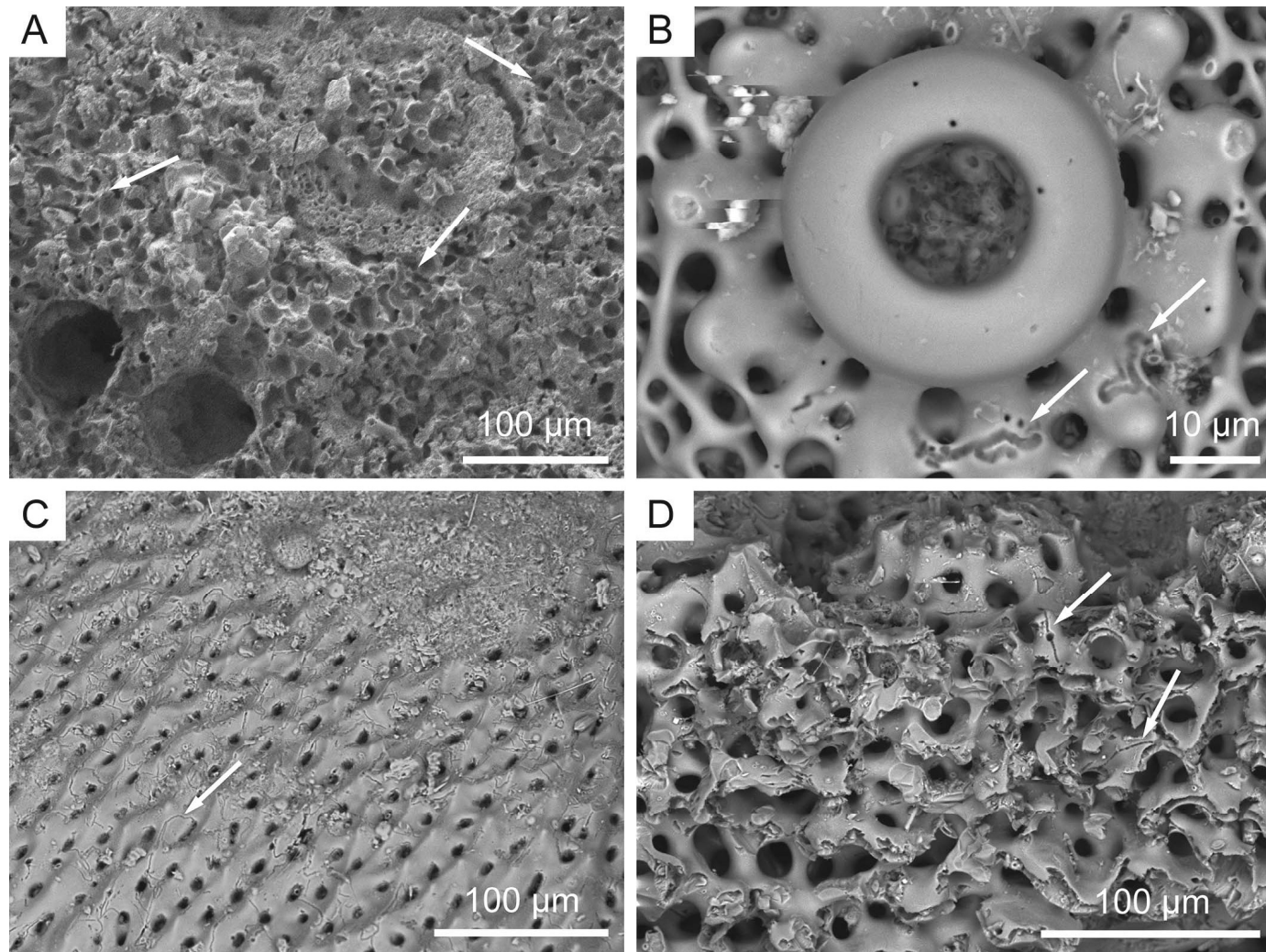


FIG. 9.—SEM images of micro-borings in *Echinocyamus* tests from the Tasmanid Seamounts. **A**) Stereom with potential sponge or fungal excavations (specimen TMD-25-SM130-5). **B**) Tubercle with potential fungal micro-borings on the platform (specimen TMD-25-SM130-8). **C**) Stereom with micro-borings throughout the surface (specimen TMD-25-SM130-11). **D**) Stereom showing excavations with rows of micropores (specimen TMD-25-SM130-6). White arrows indicate micro-borings.

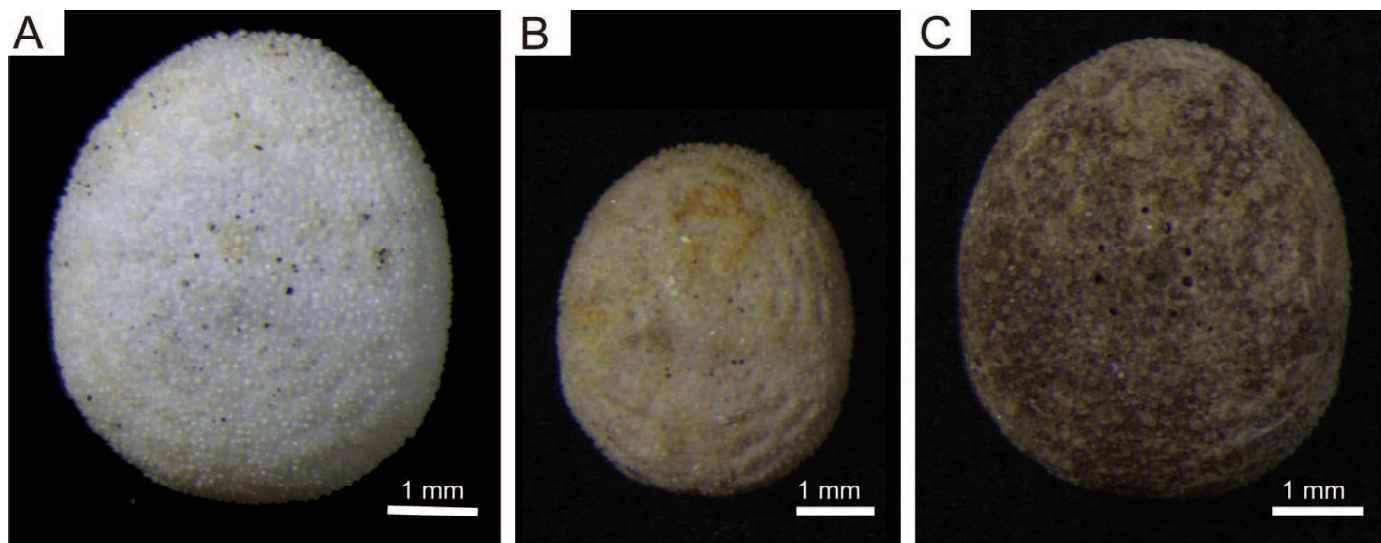


FIG. 10.—Photographs of *Echinocymus* tests showing the three staining categories. A) Not stained. B) Moderately stained. C) Dark stained. All individuals collected from dredge TMD-25.

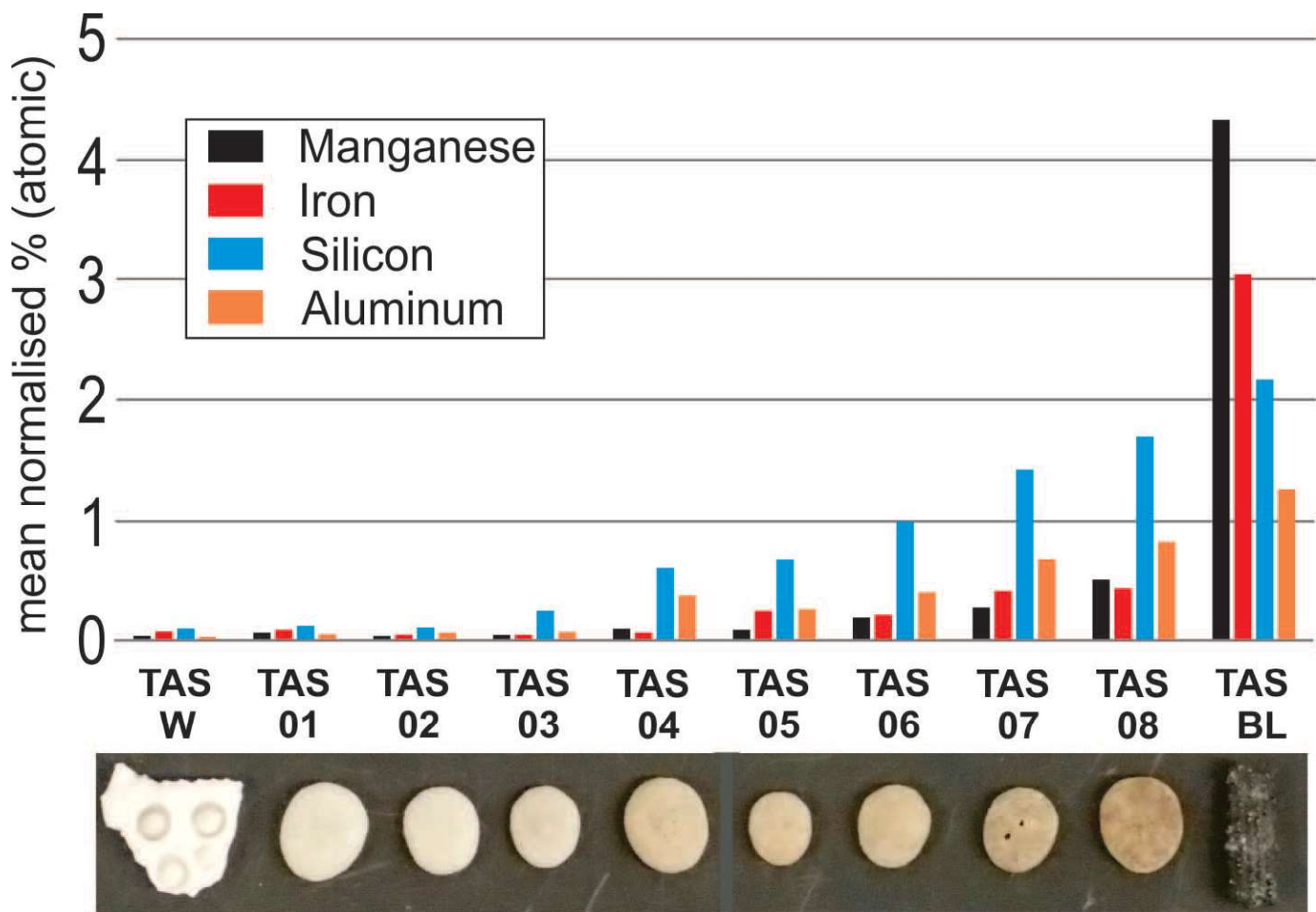


FIG. 11.—Plot of mean normalized EDS data for Mn, Fe, Si, and Al for eight *Echinocymus* samples for dredge TMD-25 along with a fresh echinoid fragment and a stained echinoid spine. Note the increase in element concentration with staining and that the Fe and Mn values vary in an inconsistent way whereas the Al and Si values increase systematically.

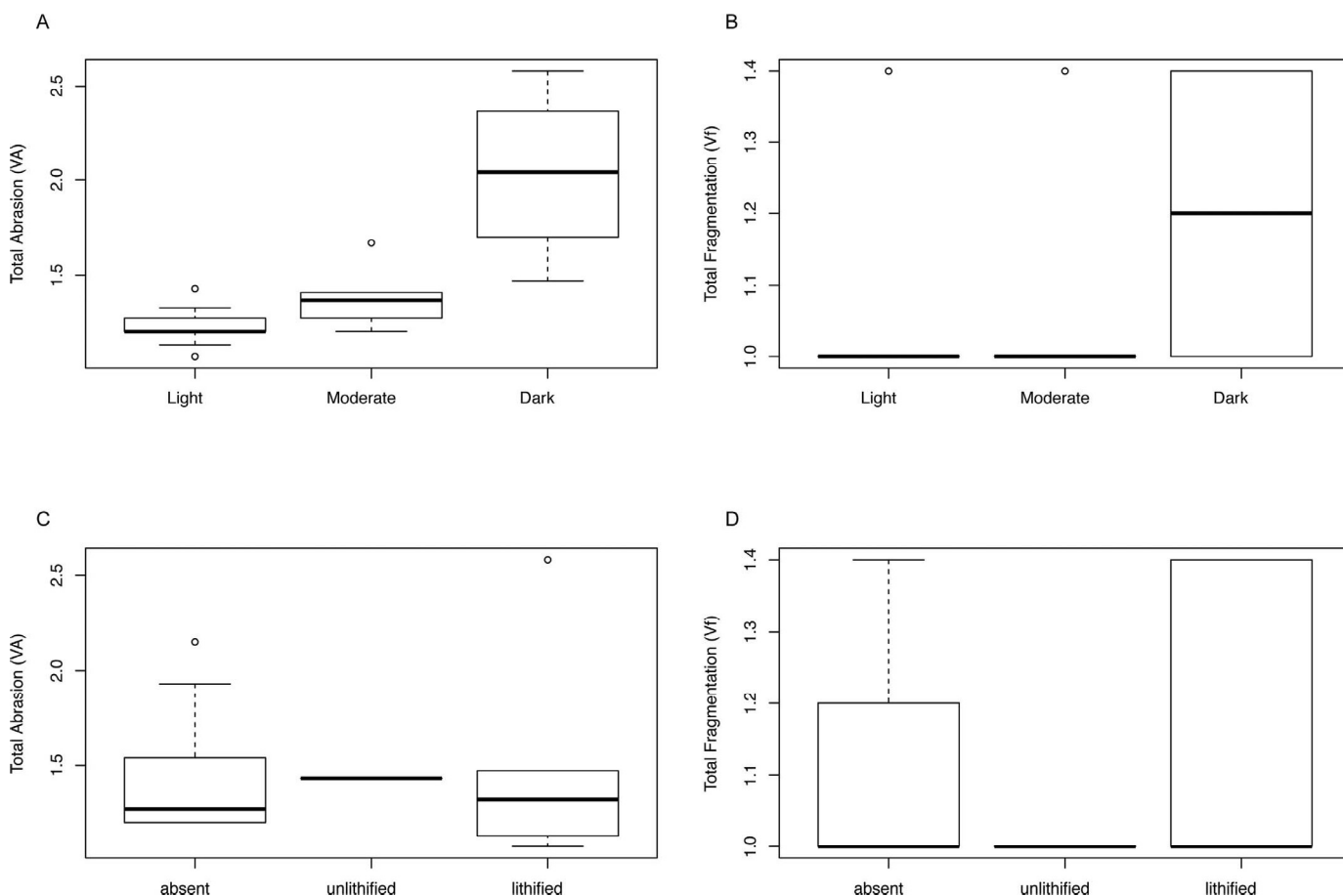


FIG. 12.—Box-plots of taphonomic alterations. **A)** Total abrasion for three categories of staining. Highly stained (dark) tests show higher abrasion values than less stained tests. **B)** Fragmentation for three categories of staining. Fragmented tests are darker stained than non-fragmented specimens. **C)** Total abrasion for three categories of lithification. Abrasion values are similar between lithification grades. **D)** Fragmentation for three categories of lithification. Highest fragmentation is visible in non-filled tests and tests filled with lithified sediment.

sea settings might be increased compared to those of shallow-water environments (Grun and Nebelsick 2016) due to an extended residence time of skeletal remains on the seafloor (Voight and Walker 1995). Phototrophic bioeroders such as endolithic cyanobacteria dominate in shallow environments but are absent at aphotic depths. In deep-sea settings, heterotrophic organisms such as fungi, sponges, foraminifers, annelids, and bacteria are the main bioeroders (Radtke et al. 1997; Gektidis 1997; Vogel et al. 1999, 2000; Beuck et al. 2010; Wisshak 2012; Golubic et al. 2019).

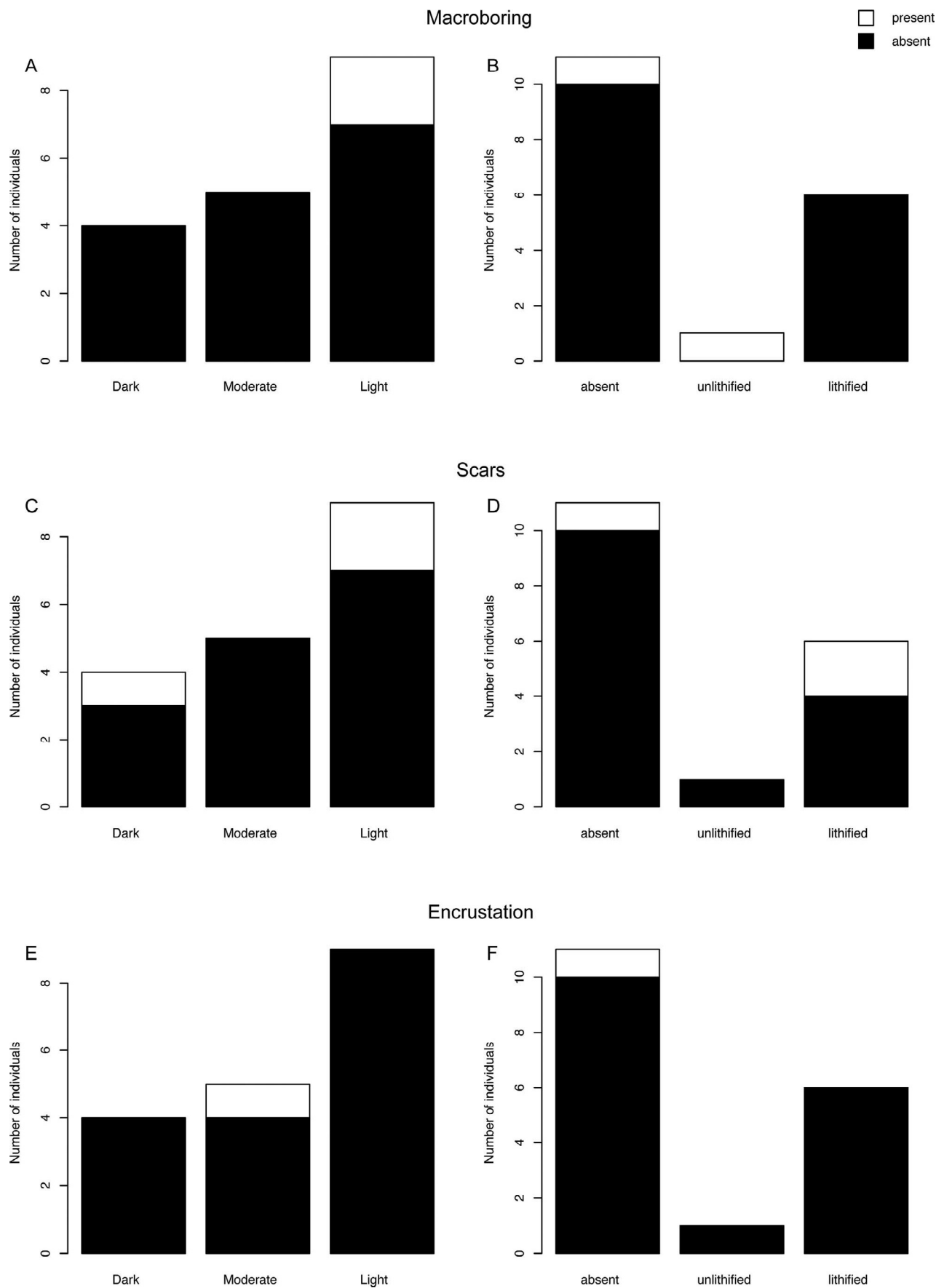
Depressions

Depressions in the deep-sea specimens (Fig. 7B, 7C) are rare and of unknown origin. Possible origin of depressions includes predatory attacks, trauma, and ontogenetic malformation. Differentiation between depressions and other traces can be difficult. For example, a scar on the surface can resemble a figure-eight shaped boring in earliest stages (Fig. 7C). This scar, however, is interpreted as the result of two abraded tubercles in proximity rather than a biotic boring.

Staining

Although taphonomic staining is common in deep-sea settings with many skeletons eventually taking on a dark stain, it has been the focus of relatively little study. Staining processes are typically the result of chemical alteration with precipitation of authigenic minerals and are time dependent

(e.g., Tomašových et al. 2017). Hence, staining grades can be used as an approximation for test exposure time on the seafloor or relative age of a sample with the least stained samples generally representing the least time. The strong correlation between Mn and Fe in the samples suggests that some part of the staining is caused by Mn and Fe oxides, which are abundant in many of the Tasmanid Seamount dredges. Crusts of black oxides containing Mn and Fe are abundant in many deep sea settings where they may form above or below the sediment-water interface with common growth rates of 1 to 7 mm/My (Hein and Koschinsky 2014). Heavily Fe-Mn oxide stained deep sea corals have been recovered by dredging and dated to > 10,000 yrs using U-series techniques (Edinger and Sherwood 2012), but staining also has been shown to start forming very early, in some cases owing presumably to microbial influence within biofilms (e.g., Freiwald and Wilson 1998). Those authors found that initial Fe-Mn staining began on the surface of live coral skeletons even where protected beneath soft tissue, but that more intense staining occurred once the tissue was removed, but while living corallites were still present. Hence staining may occur relatively rapidly relative to the long lifespans of some deep sea corals (Edinger and Sherwood 2012). The role of bacteria in Fe and Mn oxidation in deep sea crusts and films is controversial (Wang and Müller 2009; Wang et al. 2009; Hein and Koschinsky 2014; Jiang et al. 2017), but provides additional complications for interpreting the pathways, and especially the timing, of stain development. Thus, for redox sensitive staining the darkest tests may have experienced the greatest amount of time near the redox boundary within shallow sediments where anoxic pore



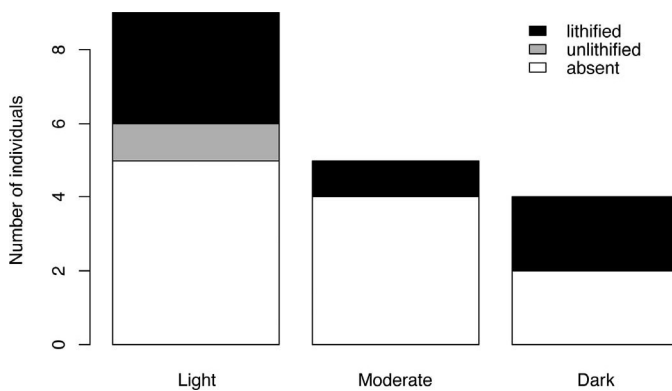


FIG. 14.—Relationship between test staining and lithification grade of test filling in *Echinocyamus*. Lithification of sediment filling occurs in all staining categories but is most abundant in lightly stained tests. Unlithified sediment filling only occurs in lightly stained tests.

waters and oxygenated seawater can mix. This zone may extend to the seafloor where oxidation is controlled within bacterial biofilms. Hence, Fe-Mn oxide staining rates will be a function of local redox kinetics, sedimentation rate, bioturbation rate, disturbance rate and, most importantly, time.

Other staining mechanisms in the deep sea include growth of authigenic clays and goethite (Tomašových et al. 2017) and the strong correlation of Si and Al in the present samples is consistent with the presence of authigenic clays. Discoloration produced by authigenic clays and goethite was found to form on nautiloid shells within ~ 200 years in mesobathyal depths but at longer, millennial time scales for shells at epibathyal depths (Tomašových et al. 2017). The relatively poor correlation of Fe and Si on the present data does not support the abundance of Fe-rich clays, but the decoupling of Fe and Mn concentrations within the *Echinocyamus* data suggests the possibility of additional Fe-rich phases, such as goethite. Unfortunately, the mineralogy cannot be analyzed directly by x-ray diffraction, as the samples are too small, but the consistent increase in Si and Al concentration with staining (Fig. 11) suggests that the clays are authigenic. Bleaching tests suggest that observed staining does not have a high organic content. Regardless, staining in the samples, although representing a complex group of processes, suggests that this feature can be used as a relative measure of residence time on or near the seafloor.

Filling

The degree of filling and lithification of the sediment in the echinoid test (Fig. 8) can be used as an indicator of burial. A filled test where the sediment is lithified most likely was buried in this sediment for relatively long time. A test filled with unlithified sediment was likely buried for a shorter time. Non-filled tests either have not been buried or lost their filling over time or during processing. Cementation on the seafloor was found to enhance the preservation of delicate brachiopod shells in the Red Sea (Tomašových and Zuschin 2009). However, based on our data, there is no

evidence that filling, or lithification had a positive or negative effect on the preservation potential or staining of the test.

Pore filling was not recorded in the study from shallow-marine environments, but the high prevalence of pore filling in the deep-sea is probably related to the presence of finer sediment compared to shallow, higher energy environments.

Fragmentation

The low fragmentation rates and high abrasion values in the deep-sea samples indicate that tests are not prone to disarticulation due to water or sediment agitation as reported by Grun and Nebelsick (2016) for shallow-water samples (Fig. 3B). In contrast to the high-energy environments of the Mediterranean Sea (Grun and Nebelsick 2016), deep-sea environments are typically subject to much lower energy levels and thus tests are more frequently preserved in increasing alteration states. Detrimental bioturbation can occur in both environmental settings and may contribute to the differences in fragmentation rates.

Plate-loss in the apical system is interpreted to occur post-mortem. Morphology of the hole and the clear correlation to inter-plate disarticulation is distinctive from predatory attacks, which would result in more complex fragmentation patterns with associated traces. Plate loss in both shallow-marine and deep-sea settings may be related to abrasion, which leads to a thinning of the test and plate sutures with an eventual loss of the plate.

Encrustation

Tests of echinoids in soft-bottom environments have been described as small benthic islands where organisms can attach (Belaústequi et al. 2012). The deep-sea *Echinocyamus* specimens had no epibionts attached to their skeletons, but traces indicate that they did serve as benthic islands (Fig. 15). For example, remains of possible holdfast structures were interpreted from surface features (Fig. 15A). Based on the macro-boring morphology (Figs. 7A, 8A), lithophagous bivalves may have utilized the test as habitat. Biofilms were present on both deep-sea and shallow water samples of *Echinocyamus* but differ in their composition. Biofilms on tests from the deep-sea samples contain predominantly coccoliths (Fig. 15C). Coccoliths also can occur in shallow-water biofilms (Hauser et al. 2008) but shallow biofilms more commonly contain benthic diatoms and cyanobacteria reflecting the photic conditions in their respective environment. Coccoliths contained within deep-sea biofilms have been implicated in the localized oxidation of Fe and Mn (Wang et al. 2009; Tomašových et al. 2017), finally resulting in thick Fe-Mn crusts, but there is no evidence to link staining of the present samples to that process. Coccoliths are ubiquitous in the ooze and most likely became trapped in the test biofilms as abundant ambient fine sediment.

Taphonomic Pathways

Due to small sample size only certain characteristics of taphonomic pathways can be determined, especially in comparison to those documented from shallow settings. Abrasion patterns on *Echinocyamus* from the deep-sea survey indicate long survival times of the tests on the sea floor. During that time of exposure, it is very likely that lithophagous and epibenthic organisms such as sponges, and fungi attached to the skeletons

FIG. 13.—Overview of taphonomic alterations in relation to three categories of test staining (A, C, E) and sediment filling / lithification (B, D, F). **A**) Macro-borings in relation to test staining. Light-stained tests more often contain macro-borings. **B**) Macro-borings in relation to filling and lithification. Unfilled or unlithified tests contain macro-borings. **C**) Scars or depressions in relation to test staining. Dark and light stained tests contain scars or depressions. **D**) Scars or depressions in relation to filling and lithification. Unfilled or tests with lithified sediment filling contain scars and depressions. **E**) Encrustation in relation to test staining. Moderately stained tests show signs of encrustation. **F**) Encrustation in relation to filling and lithification. Unfilled tests show signs of encrustation.

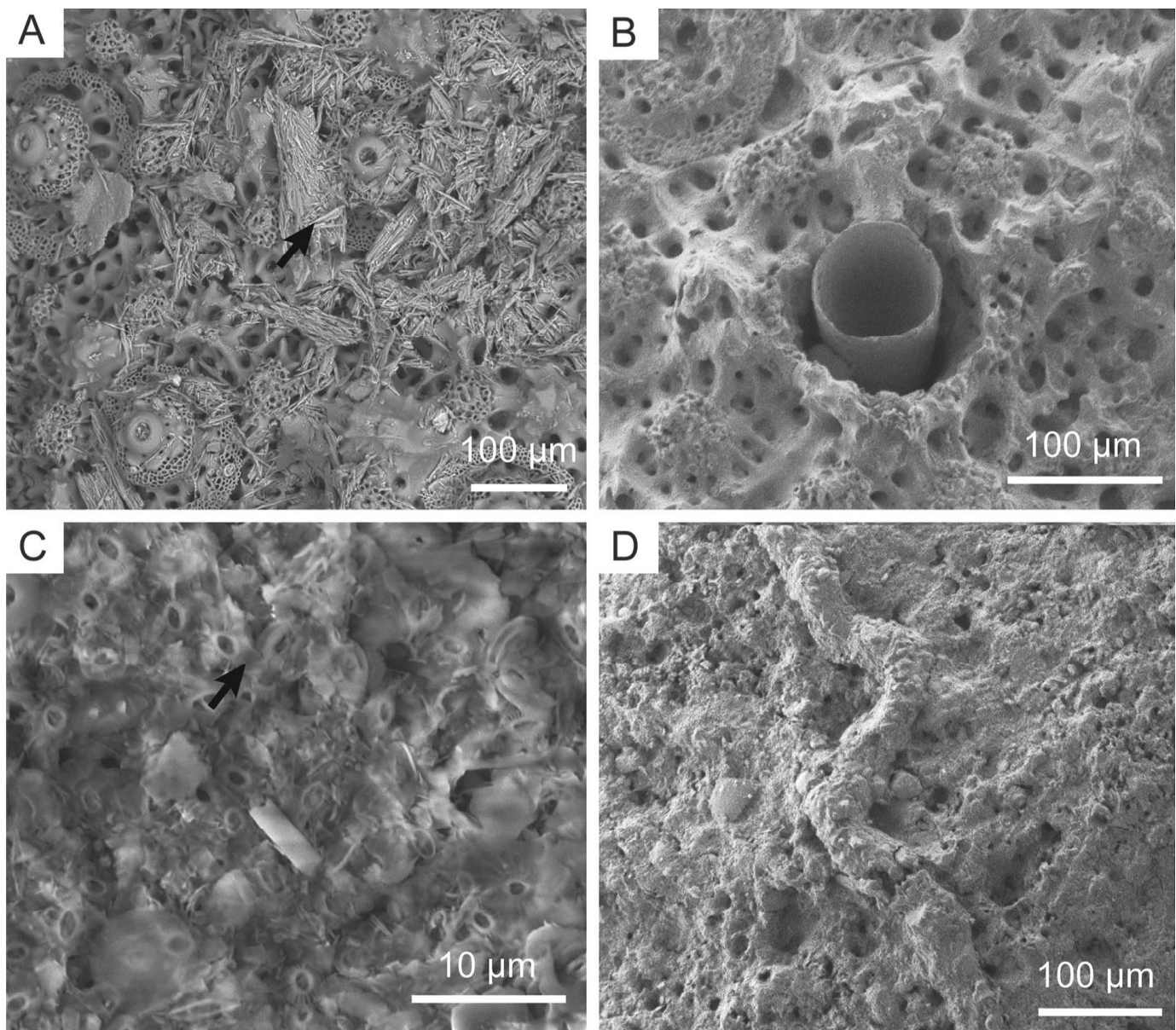


FIG. 15.—SEM images of encrusted *Echinocymus* test surfaces. **A**) Aragonite needles likely stem from an incipient holdfast or microbialite (specimen TMD-25-SM130-6). **B**) A tube penetrating the test (specimen TMD-25-SM130-3). **C**) Biofilm with bound coccoliths (specimen TMD-15-SM241). **D**) Microtube in biofilm (specimen TMD-15-SM241).

and used them as benthic secondary hard substrates in a soft-bottom environment. The soft-bottom habitat leads to sediment-filling of the tests over time, which can be preserved in the form of lithified and non-lithified fillings depending on the sediment composition and time frame of filling. The longer the time of exposure of *Echinocymus* tests in the deep-sea environment, the more likely would be plate loss due to water and sediment agitation, bioerosion or bioturbation. The time of test exposure in the environment also dictates filling and staining levels.

CONCLUSION

This study is the first analysis of taphonomic alteration patterns on the clypeasteroid echinoid genus *Echinocymus* from deep-sea seamounts off

the coast of Australia. By comparing the taphonomic alteration on tests of *Echinocymus* from these deep-sea environments with previously published research on taphonomic patterns in *Echinocymus* from shallow-water environments, we show differences and similarities in taphonomic test alteration in these environmental settings. Deep-sea and shallow-water samples were both generally abraded, but with greater pore abrasion in the deep-sea setting. Deep-sea macro-borings differ distinctly in morphology from any reported predatory or parasitic borings in this genus. However, these borings are most likely a biotic result, resembling borings of lithophagous bivalves or nematodes. Micro-borings are likely the result of sponge and/or fungal activity, rather than the cyanobacteria common in shallower settings. Depressions present in some tests have unclear origins. Staining is a result of chemical alteration of the test

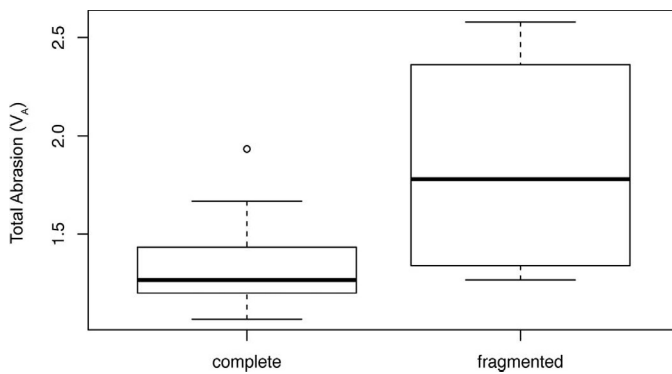


FIG. 16.—Box-plot comparison of the total abrasion value of deep-sea *Echinocymus* samples between complete and fragmented tests. Fragmented specimens show higher abrasion values than complete specimens.

surface, but its exact nature is not clear. Darker stained specimen show higher abrasion patterns than less stained tests. Filling is present as loose or lithified sediment. The degree of filling is unrelated to the preservation of the test. Fragmentation is low in the deep-sea environment, which reflects low sediment and water agitation rates.

ACKNOWLEDGMENTS

We thank Captain Michael Watson, Benjamin Cohen and the technical and scientific crew of the R/V Southern Surveyor for their expertise and support during MNF cruise ss2012-v078 and the CSIRO Marine National Facility for funding ship-time. Australian Geographic, Geological Society of London, Jeremy Willson Charitable Trust, Inter Ridge, Marine Geoscience Organisation of Australia and the UQ Dorothy Hill Professorship provided additional funding to support the fieldwork. Tobias B. Grun's work was partly supported by National Science Foundation grants EAR SGP-1630475 and EAR SGP-1630276. James Sadler helped sort sediments on board. Mihaljević's research was supported by the Robert Day Postdoctoral Fellowship at The University of Queensland; thus, immense gratitude goes to Robert Day himself. Dr. Carlos Spier helped with EDS analysis. We are thankful to James Nebelsick, Martin Zuschin, Adam Tomasovich and two anonymous reviewers for their constructive comments.

SUPPLEMENTAL MATERIAL

Data are available from the PALAIOS Data Archive: <https://www.sepm.org/supplemental-materials>.

REFERENCES

ALVE, E. and MURRAY J.W., 1997, High benthic fertility and taphonomy of foraminifera: a case study of the Skagerrak, North Sea: *Marine Micropaleontology*, v. 31, p. 157–175, doi: 10.1016/S0377-8398(97)00005-4.

AUSICH, W.I., 2001, Echinoderm taphonomy, in M. Jangoux and J.M. Lawrence (eds.), *Echinoderm Studies*, 6: Balkema, Lisse, p. 171–227.

BAUMILLER, T.K., 2003, Experimental and biostratinomic disarticulation of crinoids: taphonomic implications, in J.-P. Féral et al. (eds.), *Echinoderm Research 2001: Proceedings of the Sixth European Conference on Echinoderm Research*, Banyuls-sur-mer, 3–7 September 2001, p. 243–248.

BATHURST, R.G.C., 1967, Depth indicators in sedimentary carbonates: *Marine Geology*, v. 5, p. 447–471, doi: 10.1016/0025-3227(67)90053-9.

BELAÚSTEGUI, Z., DE GIBERT, J.M., NEBELSICK, J.H., DOMÉNECH, R., and MARTINELL, J., 2012, Clypeasteroid echinoid tests as benthic islands for gastrochaenid bivalve colonization: evidence from the middle Miocene of Tarragona, north-east Spain: *Palaeontology*, v. 56, p. 783–796, doi: 10.1111/pala.12010.

BEST, M.M.R., 2008, Contrast in preservation of bivalve death assemblages in siliciclastic and carbonate tropical shelf settings: *PALAIOS*, v. 23, p. 796–809.

BEUCK, L., FREIWALD, A., and TAVIANI, M., 2010, Spatiotemporal bioerosion patterns in deep-water scleractinians from off Santa Maria di Leuca (Apulia, Ionian Sea): *Deep-Sea Research Part II*, v. 57, p. 458–470, doi: 10.1016/j.dsrr.2009.08.019.

BEUCK, L., VERTINO, A., STEPINA, E., KAROLCZAK, M., and PFANNKUCHE, O., 2007, Skeletal response of *Lophelia pertusa* (Scleractinia) to bioeroding sponge infestation visualised with micro-computed tomography: *Facies*, v. 53, p. 157–176, doi: 10.1007/s10347-006-0094-9.

BOEKSHOTEN, G.J., 1966, Shell borings of sessile epibiotic organisms as palaeoecological guides (with examples from the Dutch coast). *Palaeogeography, Palaeoclimatology, Palaeoecology*, v. 2, p. 333–379.

BRANSON, O., READ, E., REDFERN, S.A.T., RAU, C., and ELDERFIELD, A., 2015, Revisiting diagenesis on the Ontong Java Plateau: Evidence for authigenic crust precipitation in *Globorotalia tumida*: *Paleoceanography*, v. 30, p. 1490–1502, doi: 10.1002/2014PA002759.

BRETT, C.E., PARSONS-HUBBARD, K.M., WALKER, S.E., FERGUSON, C., POWELL, E.N., STAFF, G., ASHTON-ALCOX, K.A., and RAYMOND, A., 2011, Gradients and patterns of sclerobionts on experimentally deployed bivalve shells: synopsis of bathymetric and temporal trends on a decadal time scale: *Palaeogeography, Palaeoclimatology, Palaeoecology*, v. 312, p. 278–304, doi: 10.1016/j.palaeo.2011.05.019.

BROWN, S.J. and ELDERFIELD, H., 1996, Variations in Mg/Ca and Sr/Ca ratios of planktonic foraminifera caused by postdepositional dissolution: evidence of shallow Mg-dependent dissolution: *Paleoceanography*, v. 11, p. 543–551, doi: 10.1029/96PA01491.

CHAZOTTES, V., CABIOCH, G., GOLUBIC, S., and RADTKE, G., 2009, Bathymetric zonation of modern microborers in dead coral substrates from New Caledonia—implications for paleodepth reconstructions in Holocene corals: *Palaeogeography, Palaeoclimatology, Palaeoecology*, v. 280, p. 456–468, doi: 10.1016/j.palaeo.2009.06.033.

COHEN, B.E., WEBB, G., VASCONCELOS, P., KNESEL, K., and ARCUS, R., 2012, Tasmanid Seamounts: Volcanic, Tectonic, and Carbonate Record Voyage Plan Project Report: Australian Marine National Facility, 27 p.

COLLEN, J.D. and BURGESS, C.J., 1979, Calcite dissolution, overgrowth and recrystallization in the benthic foraminiferal genus *Notorotalia*: *Journal of Paleontology*, v. 53, p. 1343–1353.

CRONBLAD, H.G. and MALMGREN, B.A., 1981, Climatically controlled variation of Sr and Mg in Quaternary planktonic foraminifera: *Nature*, v. 291, p. 61–64, doi: 10.1038/91061a0.

CROSSINGHAM, T.J., VASCONCELOS, P.M., CUNNINGHAM, T., and KNESEL, K.M., 2017, 40Ar/39Ar geochronology and volume estimates of the Tasmanid Seamounts: support for a change in the motion of the Australian plate: *Journal of Volcanology and Geothermal Research*, v. 343, p. 95–108, doi: 10.1016/j.jvolgeores.2017.06.014.

DAWBER, C.F. and TRIPATI, A., 2012, Relationships between bottom water carbonate saturation and element/Ca ratios in coretop samples of the benthic foraminifera *Oridorsalis umbonatus*: *Biogeosciences*, v. 9, p. 3029–3045, doi: 10.5194/bg-9-3029-2012.

DELINE, B. and PARSONS-HUBBARD, K.M., 2013, Experimentally observed soft-tissue preservation near a marine brine seep: *Palaeontology*, v. 56, p. 893–900, doi: 10.1111/pala.12023.

DENNE, R.A. and SEN GUPTA, B.K., 1989, Effects of taphonomy and habitat on the record of benthic foraminifera in modern sediments: *PALAIOS*, v. 4, p. 414–423, doi: 10.1016/S0377-8398(97)00005-4.

DYNOWSKI, J.F., 2012, Echinoderm remains in shallow-water carbonates at Fernandez Bay, San Salvador Island, Bahamas: *PALAIOS*, v. 27, p. 181–189, doi: 10.2110/palo.2011.p11-015r.

EDINGER, E.N. and SHERWOOD, J.B., 2012, Applied taphonomy of gorgonian and antipatharian corals in Atlantic Canada: experimental decay rates, field observations, and implications for assessing fisheries damage to deep-sea coral habitats: *Neues Jahrbuch für Geologie und Paläontologie-Abhandlungen*, v. 265/2, p. 199–218, doi: 10.1127/0077-7749/2012/0255.

FREIWALD, A., 1995, Bacteria-Induced Carbonate Degradation: A Taphonomic Case Study of *Cibicides lobatulus* from a High-Boreal Carbonate Setting: *Palaios*, v. 10, p. 337–346.

FREIWALD, A. and WILSON, J.B., 1998, Taphonomy of modern deep, cold-temperate water coral reefs: *Historical Biology*, v. 13, p. 37–52, doi: 10.1080/08912969809386571.

GEKTIDIS, M., 1997, Microbioerosion in Bahamian ooids: *CFS Courier Forschungsinstitut Senckenberg*, v. 201, p. 109–121.

GIBSON, M.A. and WATSON, J.B., 1989, Predatory and non-predatory borings in echinoids from the upper Ocala Formation (Eocene), north-central Florida, USA: *Palaeogeography, Palaeoclimatology, Palaeoecology*, v. 71, p. 309–321.

GLAUB, I., VOGEL, K., and GEKTIDIS, M., 2001, The role of modern and fossil cyanobacterial borings in bioerosion and bathymetry: *Ichnos*, v. 8, p. 185–195, doi: 10.1080/10420940109380186.

GOLUBIC, S., CAMPBELL, S.E., DROBNE, K., CAMERON, B., BALSAM, W.L., CIMERMAN, F., and DUBOIS, L., 1984, Microbial endoliths: a benthic overprint in the sedimentary record, and a paleobathymetric cross-reference with foraminifera: *Journal of Paleontology*, v. 58, p. 351–361.

GOLUBIC, S., CAMPBELL, S.E., LEE, S.-J., and RADTKE, G., 2016, Depth distribution and convergent evolution of microboring organisms: *Palaeontologische Zeitschrift*, v. 90, p. 315–326, doi: 10.1007/s12542-016-0308-6.

GOLUBIC, S., PERKINS, R.D., AND LUKAS, K.J., 1975, Boring microorganisms and microborings in carbonate substrates, in R.W. Frey (ed.), *The Study of Trace Fossils*: Springer, Berlin, p. 229–259, doi: 10.1007/978-3-642-65923-2_12.

GOLUBIC, S., SCHNEIDER, J., LE CAMPION-ALSUMARD, T., CAMPBELL, S.E., HOOK, J.E., AND RADTKE, G., 2019, Approaching microbial bioerosion: Facies, v. 65, article 25, doi: org/10.1007/s10347-019-0568-1.

GORZELAK, P. AND SALAMON, M.A., 2013, Experimental tumbling of echinoderms—taphonomic patterns and implications: *Palaeogeography, Palaeoclimatology, Palaeoecology*, v. 386, p. 569–574.

GREENSTEIN, B.J., 1991, An integrated study of echinoid taphonomy: predictions for the fossil record of four echinoid families: *PALAIOS*, v. 6, p. 519–540, doi: 10.2307/3514916.

GREENSTEIN, B.J., 1993, Is the fossil record of regular echinoids really so poor? A comparison of living and subfossil assemblages: *PALAIOS*, v. 8, p. 587–601, doi: 10.2307/3515034.

GROENEVELD, J., NÜRNBERG, D., TIEDEMANN, R., REICHART, G.-J., STEPH, S., REUNING, L., CRUDELI, D., AND MASON, P., 2008, Foraminiferal Mg/Ca increase in the Caribbean during the Pliocene: Western Atlantic Warm Pool formation, salinity influence, or diagenetic overprint?: *Geochemistry, Geophysics, Geosystems*, v. 9, Q01P23, doi: 10.1029/2006GC001564.

GRUN, T.B., KROH, A., AND NEBELSICK, J.H., 2017, Comparative drilling predation on time-averaged phosphatized and nonphosphatized assemblages of the minute clypeasteroid *Echinocymus stellatus* from Miocene offshore sediments (Globigerina Limestone Formation, Malta): *Journal of Paleontology*, v. 91, p. 633–642, doi: 10.1017/jpa.2016.123.

GRUN, T.B. AND NEBELSICK, J.H., 2016, Taphonomy of a clypeasteroid echinoid using a new quasimetric approach: *Acta Palaeontologica Polonica*, v. 61, p. 689–699, doi: 10.4202/app.00200.2015.

GRUN, T.B., SCHEVEN, M. VON, BISCHOFF, M., AND NEBELSICK, J.H., 2018, Structural stress response of segmented natural shells: a numerical case study on the clypeasteroid echinoid *Echinocymus pusillus*: *Journal of The Royal Society Interface*, v. 15, p. 20180164, doi: 10.1098/rsif.2018.0164.

GRUN, T.B., SIEVERS, D., AND NEBELSICK, J.H., 2014, Drilling predation on the clypeasteroid echinoid *Echinocymus pusillus* from the Mediterranean Sea (Giglio, Italy): *Historical Biology*, v. 26, p. 745–757, doi: 10.1080/08912963.2013.841683.

HALEY, B.A., KLINKHAMMER, G.P., AND MIX, A.C., 2005, Revisiting the rare earth elements in foraminiferal tests: *Earth and Planetary Science Letters*, v. 239, p. 79–97, doi: 10.1016/j.epsl.2005.08.014.

HAMMER, Ø., HARPER, D.A.T., AND RYAN, P.D., 2001, PAST: Paleontological Statistics Software Package for Education and Data Analysis: *Palaeontologia Electronica*, v. 4, 9 p. 178 kB, http://palaeo-electronica.org/2001_1/past/issue1_01.htm. Checked August 2020.

HAUSER, I., OSCHMANN, W., AND GISCHLER, E., 2008, Taphonomic signatures on modern Caribbean bivalve shells as indicators of environmental conditions (Belize, Central America): *PALAIOS*, v. 23, p. 586–600, doi: 10.2110/palo.2007.p07-075r.

HEIN, J.R. AND KOSCHINSKY, A., 2014, Deep-ocean ferromanganese crusts and nodules, in H.D. Holland and K.K. Turekian (eds.), *Treatise on Geochemistry*, second edition: Elsevier, Amsterdam, p. 273–291.

HIGGINS, J.A., BLÄTTLER, C.L., LUNDSTROM, E.A., SANTIAGO-RAMOS, D.P., AKHTAR, A.A., CRÜGER AHM, A.-S., BIALIK, O., HOLMDEN, C., BRADBURY, H., MURRAY, S.T., AND SWART, P.K., 2018, Mineralogy, early marine diagenesis, and the chemistry of shallow-water carbonate sediments: *Geochimica et Cosmochimica Acta*, v. 220, p. 512–534, doi: 10.1016/j.gca.2017.09.046.

HIGGINS, J.A. AND SCHRAG, D.P., 2012, Records of Neogene seawater chemistry and diagenesis in deep-sea carbonate sediments and pore fluids: *Earth and Planetary Science Letters*, v. 357, p. 386–396, doi: 10.1016/j.epsl.2012.08.030.

JIANG, X.D., SUN, X.M., GUAN, Y., GONG, J.L., LU, Y., LU, R.F., AND WANG, C., 2017, Biomineralisation of the ferromanganese crusts in the Western Pacific Ocean: *Journal of Asian Earth Sciences*, v. 136, p. 58–67, doi: 10.1016/j.jseas.2017.01.025.

JONES, B. AND PEMBERTON, G., 1988, *Lithophaga* borings and their influence on the diagenesis of corals in the Pleistocene Ironshore Formation of Grand Cayman Island, British West Indies: *PALAIOS*, v. 3, p. 3–21.

KIDWELL, S.M. AND BAUMILLER, T., 1990, Experimental disintegration of regular echinoids: roles of temperature, oxygen, and decay thresholds: *Paleobiology*, v. 16, p. 247–271, doi: 10.1017/S0094837300009982.

LIPPS, J.H., 1983, Biotic interactions in benthic foraminifera, in M.J.S. Tevesz and P.L. McCall (eds.), *Biotic interactions in Recent and fossil benthic communities*: Plenum Press, New York, p. 331–376.

MORTENSEN, T., 1948, A Monograph of the echinoidea, *Clypeastroida*: CA Reitzel, Copenhagen, 471 p.

MURRAY, J.W. AND ALVE, E. 1999, Natural dissolution of modern shallow water benthic foraminifera: taphonomic effects on the palaeoecological record: *Palaeogeography, Palaeoclimatology, Palaeoecology*, v. 146, p. 195–209.

NEBELSICK, J.H., 1995, Actupalaeontological investigations on echinoids: the potential for taphonomic interpretation, in R.H. Emson, A.B. Smith, and A.C. Campbell (eds.), *Echinoderm Research*: A.A. Balkema, Rotterdam, p. 209–214.

NEBELSICK, J.H., 2020, Ecology of clypeasteroids, in J.M. Lawrence (ed.), *Sea Urchins: Biology and Ecology*: Elsevier Academic Press, London, p. 315–331.

NEBELSICK, J.H. AND KOWALEWSKI, M., 1999, Drilling predation on Recent clypeasteroids echinoids from the Red Sea: *PALAIOS*, v. 14, p. 127–144.

PALMER, M.R. AND ELDERFIELD, H., 1986, Rare earth elements and neodymium isotopes in ferromanganese oxide coatings of Cenozoic foraminifera from the Atlantic Ocean: *Geochimica et Cosmochimica Acta*, v. 50, p. 409–417, doi: 10.1016/0016-7037(86)90194-8.

PARSONS, K.M., POWELL, E.N., BRETT, C.E., WALKER, S.E., RAYMOND, A., CALLENDER, W.R., AND STAFF, G., 1997, Shelf and slope experimental taphonomy initiative (SSETI): Bahamas and Gulf of Mexico, in *Proceedings of the Eighth International Coral Reef Symposium*: Smithsonian Tropical Research Institute, Panama, v. 2, p. 1807–1812.

PARSONS-HUBBARD, K.M., BRETT, C.E., AND WALKER, S.E., 2011, Taphonomic field experiments and the role of the Shelf and Slope Experimental Taphonomy Initiative: *Palaeogeography, Palaeoclimatology, Palaeoecology*, v. 312, p. 195–208, doi: 10.1016/j.palaeo.2011.11.009.

POWELL, E.N. AND DAVIES, D.J., 1990, When is an “old” shell really old?: *Journal of Geology*, v. 98, p. 823–844.

POWELL, E.N., HU, X., CAI, W.-J., ASHTON-ALCOX, K.A., PARSONS-HUBBARD, K.M., AND WALKER, S., 2012, Geochemical controls on carbonate shell taphonomy in northern gulf of Mexico continental shelf and slope sediments: *PALAIOS*, v. 27, p. 571–584, doi: 10.2110/palo.2011.p11-116r.

QUILTY, P.G., 1993, Tasmanid and Lord Howe seamounts: biostratigraphy and palaeoceanographic significance: *Alcheringa, An Australasian Journal of Palaeontology*, v. 17, p. 27–53, doi: 10.1080/03115519308619487.

RADTKE, G., HOFMANN, K., AND GOLUBIC, S., 1997, A bibliographic overview of micro- and macroscopic bioerosion: *Courier Forschungsinstitut Senckenberg*, v. 201, p. 307–340.

RATHBURN, A.E. AND MIAO, Q., 1995, The taphonomy of deep-sea benthic foraminifera: comparisons of living and dead assemblages from box and gravity cores taken in the Sulu Sea: v. 25, p. 127–149, doi: 10.1016/0377-8398(94)00029-M.

ROBERTS, J.M., WHEELER, A.J., FREIWALD, A., AND CAIRNS, S.D., 2009, *Cold-Water Corals: The Biology and Geology of Deep-Sea Coral Habitats*: Cambridge University Press, New York, 368 p.

RONGSTAD, B.L., MARCHITTO, T.M., AND HERGUERA, J.C., 2017, Understanding the effects of dissolution on the Mg/Ca paleothermometer in planktic foraminifera: evidence from a novel individual foraminifera method: *Paleoceanography*, v. 32, p. 1386–1402, doi: 10.1002/2017PA003179.

SEXTON, P.F. AND WILSON, P.A., 2009, Preservation of benthic foraminifera and reliability of deep-sea temperature records: Importance of sedimentation rates, lithology, and the need to examine test wall structure: *Paleoceanography and Paleoclimatology*, v. 24, p. PA2208, doi: 10.1029/2008PA001650.

SMITH, A.B., 1984, *Echinoid Palaeobiology*: George Allen and Unwin, London, 190 p.

SMITH, A.B. AND KROH, A. (eds.), 2011, *The Echinoid Directory*: Electronic publication accessed June 1, 2018, <http://www.nhm.ac.uk/research-curation/projects/echinoid-directory>.

STEVENSON, A. AND ROCHA, C., 2013, Evidence for the bioerosion of deep-water corals by echinoids in the Northeast Atlantic: *Deep-Sea Research Part I*, v. 71, p. 73–78, doi: 10.1016/j.dsr.2012.09.005.

SWINCHATT, J.P. 1969, Algal boring: a possible depth indicator in carbonate rocks and sediments: *Bulletin of the Geological Society of America*, v. 80, p. 1391–1396, doi: 10.1130/0016-7606(1969)80[1391:ABAPDI]2.0.CO;2.

TACHIKAWA, K., TOYOFUKU, T., BASILE-DOELSCH, I., AND DELHAYE, T., 2013, Microscale neodymium distribution in sedimentary planktonic foraminiferal tests and associated mineral phases: *Geochimica et Cosmochimica Acta*, v. 100, p. 11–23, doi: 10.1016/j.gca.2012.10.010.

TOMAŠOVÝCH, A., SCHLÖGL, J., BIROŇ, A., HUDAČKOVÁ, N., AND MIKUŠ, T., 2017, Taphonomic clock and bathymetric dependence of cephalopod preservation in Bathyal, sediment-starved environments: *PALAIOS*, v. 32, p. 135–152, doi: <http://dx.doi.org/10.2110/palo.2016.039>.

TOMAŠOVÝCH, A. AND ZUSCHIN, M., 2009, Variation in brachiopod preservation along a carbonate shelf-basin transect (Red Sea and Gulf of Aden): environmental sensitivity of taphofacies: *PALAIOS*, v. 24, p. 697–716, doi: 10.2110/palo.2009.p09-018r.

VAN DER KOOL, B., IMMENHAUSER, A., STEUBER, T., BAHAMONDE RIONDA, J.R., AND MERINO TOME, O., 2010, Controlling factors of volumetrically important marine carbonate cementation in deep slope settings: *Sedimentology*, v. 57, p. 1491–1525, doi: 10.1111/j.1365-3091.2010.01153.x.

VOGEL, K., BALOG, S.J., BUNDSCUH, M., GEKTIDIS, M., GLAUB, I., KRUTSCHINNA, J., AND RADTKE, G., 1999, Bathymetrical studies in fossil reefs, with microendoliths as paleoecological indicators: *Profil*, v. 16, p. 181–191.

VOGEL, K., GEKTIDIS, M., GOLUBIC, S., KIENE, W.E., AND RADTKE, G., 2000, Experimental studies on microbial bioerosion at Lee Stocking Island, Bahamas and One Tree Island, Great Barrier Reef, Australia: implications for paleoecological reconstructions: *Lethaia*, v. 33, p. 190–204, doi: 10.1080/00241160025100053.

VOIGHT, J.R. AND WALKER, S.E., 1995, Geographic variation of shell biotits in the deep-sea snail *Gaza*: Research Part I: Oceanographic Research Papers, v. 42, p. 1261–1271, doi: 10.1016/0967-0637(95)00063-C.

WALKER, S.E. AND VOIGHT, J.R., 1994, Paleoecologic and taphonomic potential of deep sea gastropods: PALAIOS, v. 9, p. 48–59, doi: 10.2307/3515078.

WANG, X.H. AND MÜLLER, W.E.G., 2009, Marine biominerals: perspectives and challenges for polymetallic nodules and crusts: Trends in Biotechnology, v. 27, p. 375–383, doi: 10.1016/j.tibtech.2009.03.004.

WANG, X.H., SCHLOßMACHER, U., NATALIO, F., SCHRÖDER, H.C., WOLF, S.E., TREMEL, W., AND MÜLLER, W.E.G., 2009, Evidence for biogenic processes during formation of ferromanganese crusts from the Pacific Ocean: implications of biologically induced mineralization: Micron, v. 40, p. 526–535, doi: 10.1016/j.micron.2009.04.005.

WISCHAK, M., 2012, Microbioerosion, in D. Knaust and R. Bromley (eds.), Trace Fossils as Indicators of Sedimentary Environments: Developments in Sedimentology 64: Elsevier, Amsterdam, p. 213–243.

WISCHAK, M., BERNING, B., JAKOBSEN, J., AND FREIWALD, A., 2015, Temperate carbonate production: biodiversity of calcareous epiliths from intertidal to bathyal depths (Azores): Marine Biodiversity, v. 45, p. 87–112, doi: 10.1007/s12526-014-0231-6.

ZIOTNIK, M. AND CERANKA, T., 2003, Traces of cassid predation upon echinoids from the middle Miocene of Poland, v. 48, p. 491–496.

Received 11 April 2019; accepted 8 September 2020.